Lappeenranta University of Technology
School of Engineering Science
Master's Programme in Computational Engineering and Technical Physics
Intelligent Computing Major

Master's Thesis

Nikita Anisimov

KNOT DETECTION FROM LASER POINT CLOUDS FOR MULTIMODAL MATCHING OF WOODEN MATERIAL

Examiners: Prof. Heikki Kälviäinen
PhD Roman Malashin

Supervisors: D.Sc Tuomas Eerola
Prof. Lasse Lensu
Prof. Heikki Kälviäinen
Prof. Heikki Haario

ABSTRACT

Lappeenranta University of Technology
School of Engineering Science
Master's Programme in Computational Engineering and Technical Physics
Intelligent Computing Major

Nikita Anisimov

Knot detection from laser point clouds for multimodal matching of wooden material

Master's Thesis

2017

58 pages, 43 figures, 4 tables.

Examiners: Prof. Heikki Kälviäinen
PhD Roman Malashin

Keywords: computer vision, image processing, multimodal matching, laser scanning, X-ray tomography, sawmilling process, defects on logs

The goal of this thesis is to establish the effectiveness of using the laser scanning for detecting knots for the task of tracking wood for the sawing process. This thesis describes the method of detecting wooden knots from point cloud images of debarked logs by analyzing the stem surface images. To convert the 3-D log surface data to the 2-D image of the surface, every cross-section of the log was fitted by a circle. Radial distances were calculated between circle and log surface points to unroll the log surface onto a 2-D coordinate space. Areas with elevated height above the approximated cylinder surface were identified as areas of the alleged location of the knots. The results were evaluated by using data obtained from the X-ray scanning of the log and it was shown that the detection results correspond well with the true knot cluster locations computed using the X-ray data. Further, the information about the knot positions can be used to match logs and sawn boards.

PREFACE

This project helped me to better understand the principle of working in a team, as well as improve my skills. I would like to thank my supervisors and colleagues for help. I also thank my family and friends who supported all the time working on the project.

I hope you enjoy your reading.

Lappeenranta, May 24, 2018

Nikita Anisimov

CONTENTS

LIST OF ABBREVIATIONS

1-D	One-dimensional
2-D	Two-dimensional
3-D	Three-dimensional
CT	Computed Tomography
ICP	Iterative Closest Point
MATLAB	MAtrix LABoratory
RANSAC	RANdom SAmple Consensus
RFID	Radio Frequency Identification
RGB	Red, Green, Blue
RMS	Root Mean Square
SSD	Sum of Squared Intensity Differences

1 INTRODUCTION

1.1 Background

Sawmill production is a large multi-level process, and each step of this process depends on many factors. Having enough reliable information, these factors can be changed in order to increase the productivity of the enterprise. To obtain information, reliable control of each stage of production is required. That is why there was a need for an information system connecting all the production steps of the mill so that it is possible to track the life cycle of a raw material from the beginning to the end product. For sawmill production, this means that it is necessary to track all the processes of converting a log into planks and boards. [1]

The purpose of this work is to create a system for tracking knots on the point clouds images of the debarked log for solving the task of multimodal matching of raw material (logs) and the final product (sawn timber). The information about the log is obtained from laser and X-ray Computed Tomography (CT) scans. Information about the boards obtained after sawing is stored in Red, Green and Blue (RGB) images. An example images are shown in Fig. 1. Also in this paper, the efficiency of using laser scanning in comparison with the X-ray scanning for the detection of knots and clusters of knots is considered. [2]

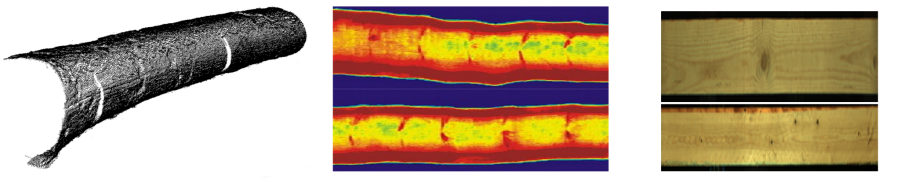

Figure 1. Image data with different modalities from different production steps of a sawmill.

This master's thesis is a part of the DigiSaw research project [2]. The DigiSaw research project targets on enhancement the productivity of sawmill industry using modern digital technologies and computer vision methods.

1.2 Objectives and delimitation

The aim of this work is to create a system capable of locating knots position on a surface of the debarked log. The objectives are as follows:

1. Analyze the data and propose a method for detecting knots.
2. Based on the selected method, design and implement the required system.
3. Evaluate the performance of the system by using the available data.
4. Make a review of possible approaches for multimodal matching of wooden material.

Due to the difficulties encountered related to the workload and the timing of the receipt of the data, the multimodal matching was not implemented in this work. However, the main aspects of the multimodal matching have been disassembled in the work to indicate further possible work on this topic.

1.3 Structure of the thesis

The thesis is organized as follows. Chapter 2 discusses the main provisions related to sawing wood and general methods of knots detection. Chapter 3 explores methods for detecting various types of defects, including knots, from laser scanning images. Different approaches of multimodal matching are introduced in Chapter 4. Chapter 5 describes in detail the approach used in this paper. Chapter 6 presents the results obtained in the course of this work. In Chapter 7 discussions are made about the possible future of the project. Finally, in Chapter 8 a conclusion is drawn from the work done.

2 SAWMILLING

2.1 Process steps

The sawmilling is the process of cutting logs into lamber. Sawmill's basic operations remain unchanged, although they vary in each enterprise. The steps of the cutting process depend on the desired final material - most often these are boards of various sizes, but also sawdust and wooden chips can be obtained. Sawing also differs in the automation production degree, as well as the quality of the raw material. The main steps of sawmillinging process are shown in Fig. 2.

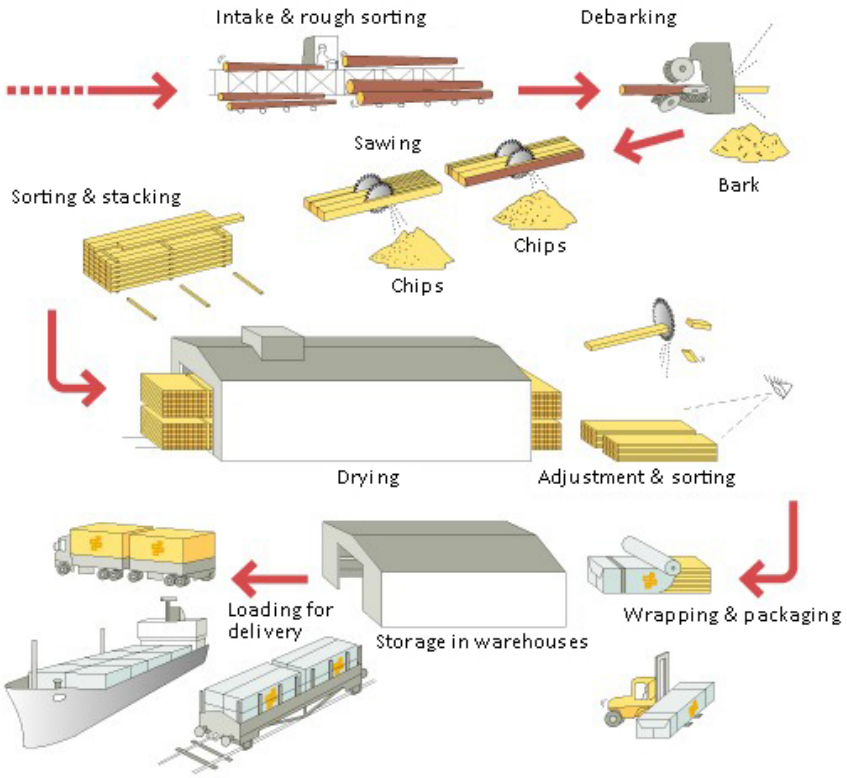

Figure 2. Sawmill process steps. [3]

The first step is debarking. At this stage, the log is cleared of the bark and rhizomes, as they complicate the process of sawing. Root reduction prevents possible difficulties, and at the same time gives the stock a more cylindrical shape. Simultaneously, most of the impurities and damages that could have occurred during transportation of the log are removed. [1]

It is customary to distinguish four types of debarking machines. Drum debarker consists of large drum that is filled with logs. The drum rotates, and the logs bang against each other. The combination of friction and the hammering action removes the bark off the stems. Flail debarkers consist of chains or other flexible materials that are whipped against stems, hammering off the bark. Inside cutter head or Rosser style debarkers the log rests upon a cradle driven by rollers that rotate the log while a rotating cutter head travels over the length of the log and removes the bark. Ring debarkers consist of a ring of cutting heads or knives that are mounted on series of arms in a circular position. They rotate around the log as it is fed through them. Machines for all four types of debarking are shown in Fig. 3. [4]

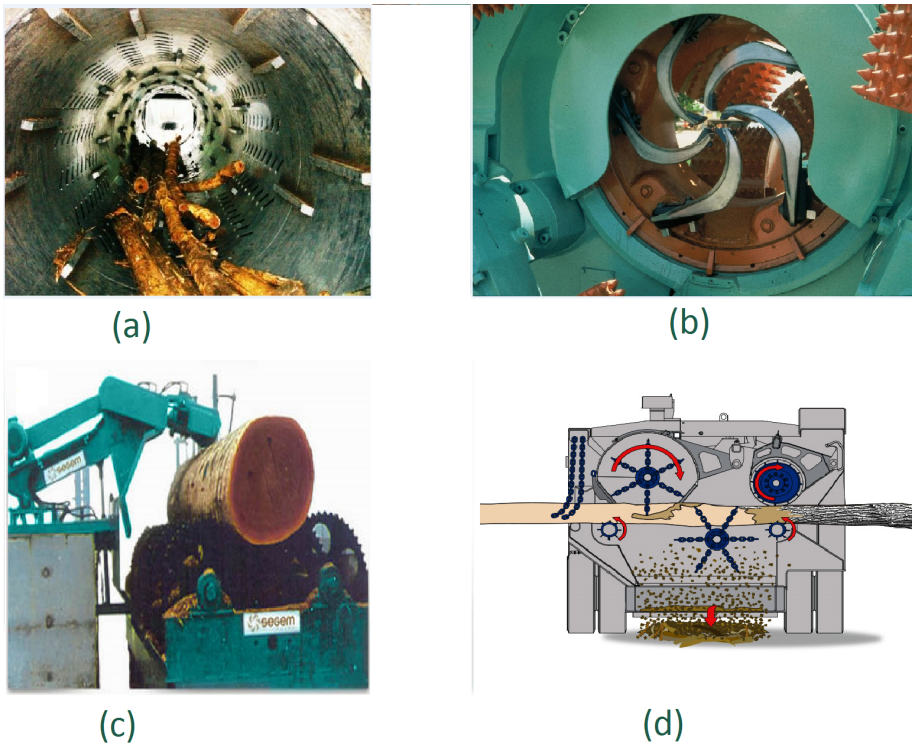

Figure 3. Different types of debarking: drum (a) [5], ring (b) [6], rosser (c) [7] and flail (d) (Modified from [8]) debarking.

The next step is sawing and cutting logs. A method used for sawing depends on both the type of wood and the desired result. The simplest method is live sawing, also known as slab sawing or through and through sawing [9]. In this case, the log is sawn along about halfway through on the opening face and then turned once to the opposite face for sawing until the log is finished. Although this can be the easiest and fastest way to cut, this results in a cupping, that is a deformation of the board caused by pith of the tree. Live sawing is generally recommended for lower quality logs because of this drawback. [10] [1]

The method of cant sawing is more preferable. Its essence is that after the first incisions the log is turned over first 180 degrees, then 90 degrees, and again 180 degrees. After each rotation, the log is sawn on one side a little more. The result of this four sides cutting is a set of boards and a square central part of the logs, which is called a cant. This cant is then split separately. Methods of live and cant sawing are shown in Fig. 4. [10]

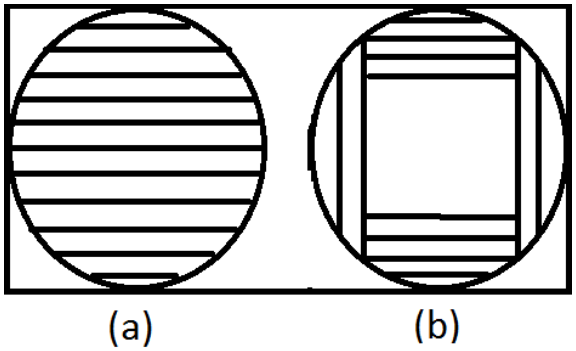

Figure 4. Sawing patterns: live (a) and cant (b). (Modified from [10])

To produce high-quality boards, the methods of tangential and radial sawing are used. These methods are shown in Fig. 5. Tangential is called a sawing method, in which the plane of the cut passes at a distance from the core, along a tangent to the annual layer of the trunk. Such boards have a pronounced texture and a saturated wave-like pattern of annual rings. Tangential cut boards have higher shrinkage and swelling rates but are more affordable. Radial sawing of wood is a method of sawing a log, in which all the fibers in the board go along the direction of the annual rings. With the radial sawing, the timber has the best physical and mechanical properties. Strength and hardness of wood with the radial cut are higher than with tangential. [11]

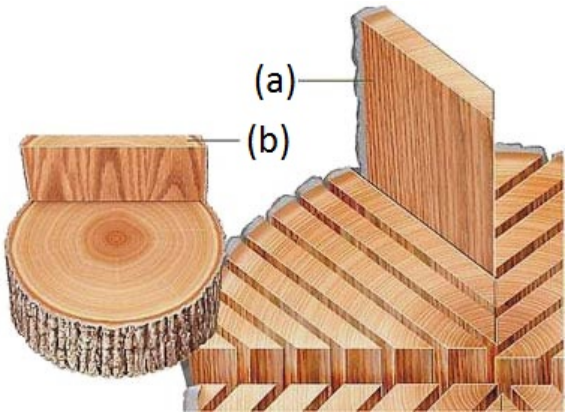

Figure 5. Types of sawing: tangential (a) and radial (b). [11]

Wood drying is the last step. This process is also called seasoning or wood lumber. Wet timber is a breeding ground for mold and pests, while dried wood does not crack, warp or deform. The wood can be dried by exposing it to the air, but this is not as effective as kiln drying. The kiln can be vacuum, solar or microwave. After drying, the wood is treated with antiseptics to protect it from moisture, temperature and pests. The resulting boards are the final product and, after selection and sorting, can be taken to a storage location. [1]

2.2 Tracing of timber

With advances in measurement technologies, it is possible to trace wood all the way from the log to a final product. Data on the state of wood obtained during the whole production process can be used to improve each step of sawmill process and tracking chain. When transporting and storing, logs are usually marked with paint or serifs. However, at the enterprise any mechanical damages of wood are extremely unhelpful and only complicate the production process. [12] [13]

More advanced methods of marking mean applying special labels and barcodes. Especially interesting is the costly and effective method based on the use of Radio Frequency Identification (RFID) technique. Its essence is to inserts a tag radially into one end of a log. On a log sorting station an RFID antenna automatically reads and identifies each log as it arrives at the sawmill by the tag ID number. However, this approach suffers from complexity and high cost of execution. More effective in terms of labor costs are tracking methods based on machine vision. [13]

The usefulness of the machine vision method for the tracking task can be seen in the example of solving the problem of the juxtaposition of boards before and after the drying process. The boards after and before drying undergo minor changes, which should be tracked. At the beginning of the process, boards pass under a line or matrix camera system for quality and dimensional measurement. In the end, after processing, boards pass under a second camera system for the final visual quality classification. Thus, it is estimated whether the drying resulted in damage to wood, for example, the appearance of a split. [14]

However, it is more effective to start tracking the log before sawing process. The laser scanning is useful for observing the shape and surface of an object. It is used on sawing to compose a three-dimensional (3-D) image of a log surface. Thus, it is possible to detect any kind of mechanical damage or natural defects from log,such as the remains of

an unearned crust or knots and branches. In turn, laser scanning of the boards reveals significant deformations and deviations of the wood after sawing or drying. [15]

X-ray tomography of logs is useful for constructing the internal structure of a log and determining its properties even before their sawing. Using computed tomography, the following defects and properties can be detected: pith, sound and dead knots, splits, resin pockets, heavy rot, slope of grain, blue stain, metals, stones, ceramics, heartwood, green density, annual rings spacing, compression wood, bark enclosures and under bark shape. With the use of special equipment, it is possible to build a 3-D internal model of the log with accurate information about the size, shape, and location of internal hardwood defects. [16] [17]

The steps for collecting data on the state of the wood are shown in Fig. 6. Even with this information, it is extremely difficult to trace logs on all sawmilling process, because after the sawing the log loses most of its distinctive features. One of the signs, the allocation of which can be useful for the task of tracking wood, can be tree rings. With the help of X-ray tomography, it is possible to obtain complete information about the rings inside the log. Other unchangeable signs can be considered knots, the structure and location of which in board can draw conclusions about the original log. This raises the question of methods for knots detection. [18]

2.3 Knot detection

Recognition with the help of machine vision allows to reliably and quickly select the properties of a log for subsequent recognition. However, many properties of logs are lost when it is processed and cut. As a result of the debarking process, information about the majority external defects, such as lesion and bark distortion, are erased. After the sawing, the data about the length, width and height of the log is distorted. However, the knots have a permanent influence on the wood, and they can be traced even after cutting.

A knot is part of the branch, enclosed in the trunk of wood. More information about the different types of knots is given in Chapter 3. The knot is the main varietal defect of timber, which is why there are many methods for tracking the position and type of knots in a log and board. The following subsections summarize are the main approaches to the detection of knots. [19]

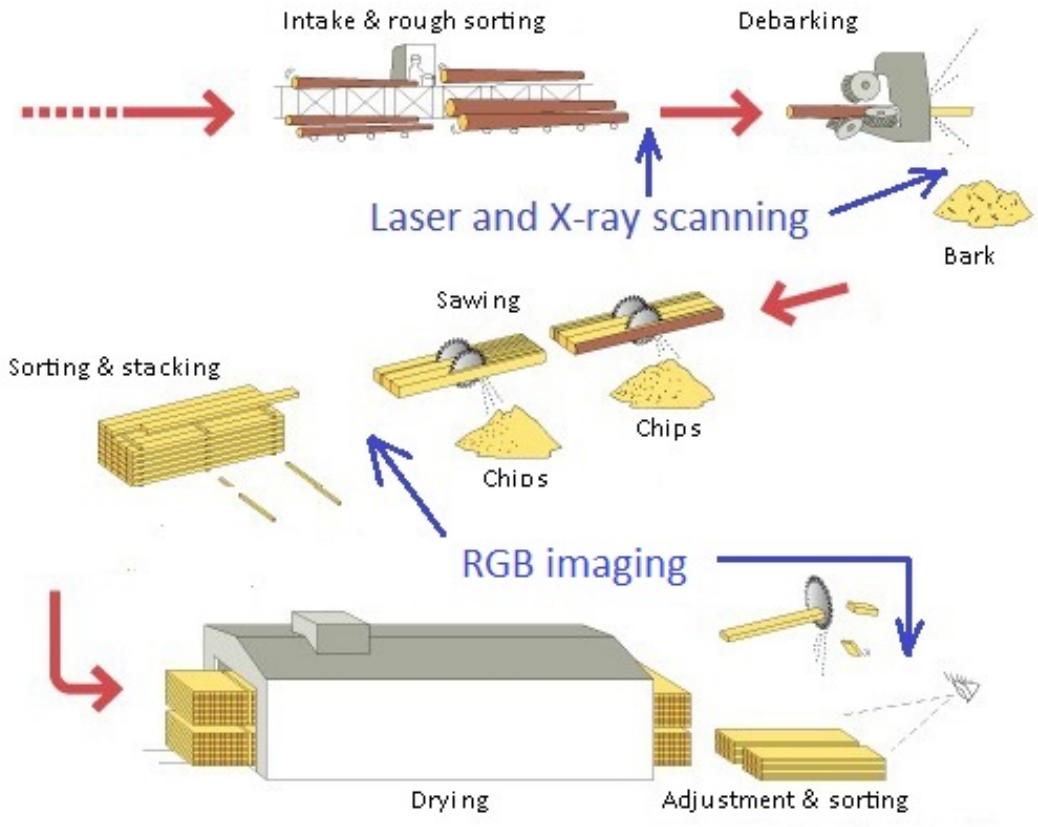

Figure 6. Sawmilling and tracking steps. (Modified from [3])

2.3.1 Knot detection from board images

Finding knots on the image of the board is a rather straightforward task. The knots strongly adhere to the wood background, and their shape and location do not significant change after drying and processing of the boards.The example of an image of a board with knots is shown in Fig. 7. This allows to effectively track the boards at this stage of the chain, using information about the number, position and dimming of the knots [17]. A suitable method for fast image alignment was implemented using two-dimensional (2-D) to one-dimensional (1-D) projection signals [14] and template matching [20].

Most methods for detecting knots with increased accuracy are based on extraction features from the image of the board. The feature set can be made by using a concept of texture and be computed from the co-occurrence matrices [21]. The image is divided into small sections, each of which is evaluated for belonging to the knot area. The conclusion is made on the basis of the value of the feature obtained at the training stage. The example of this segmentation is shown in Fig. 8. The detection system training can made by

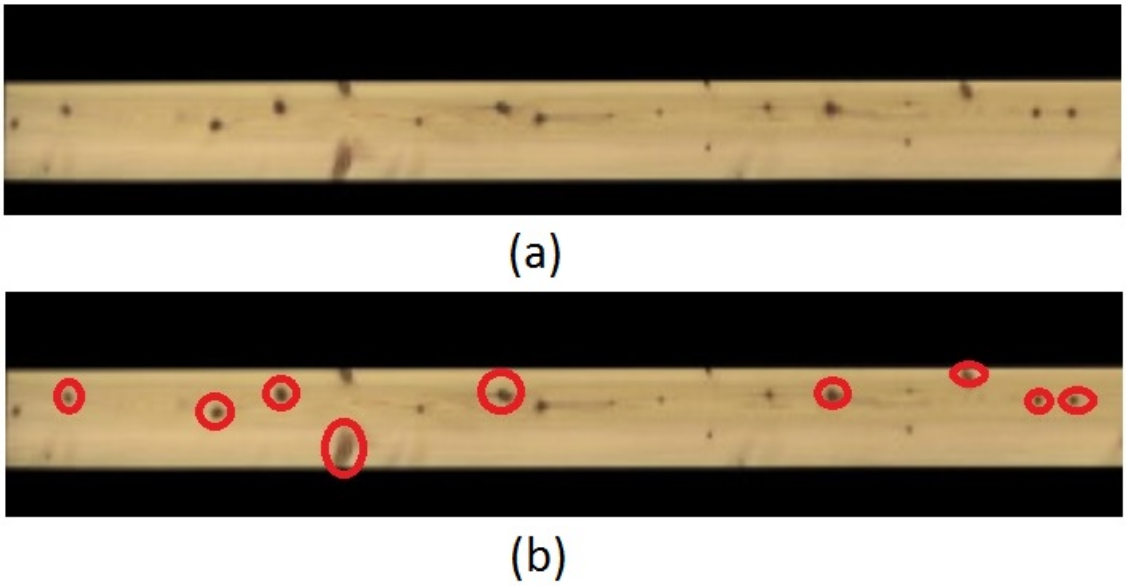

Figure 7. A rescanned boards: normal image (a) and image with highlighted knots (b). (Modified from [20])

using different machine learning paradigms, such as Neural Networks (NN) [22] [17] and Support Vector Machines (SVM) [23].

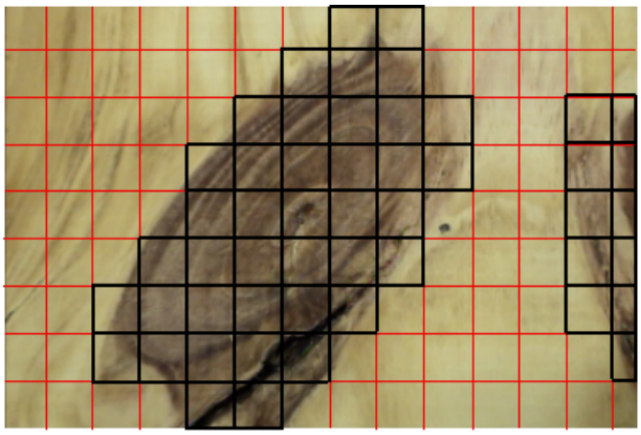

Figure 8. Board image segmented into rectangular regions (knots are highlighted). [21]

2.3.2 Knot detection from laser scans of log

Another way to detect knots is to use laser scan point cloud images of a surface of a log. According to the information on the structure and condition of the log surface, it

is possible to detect overgrown, sound and unsound knots and knot clusters, the area in which the number of knots is greater than at other places of the log [24]. Typical knot detection methods [25] have the following steps:

1. Scanning of the log.
2. Crating 3-D model of the log.
3. Detecting external surface rises and deformations.
4. Selecting knots among the found defects on the tree trunk.

The 3-D scan of a log with selected knot clusters areas is shown in Fig. 9. In more detail, the methods for detecting log surface defects, including knots, on the trunk of a tree from laser scanned data are described in Chapter 3.

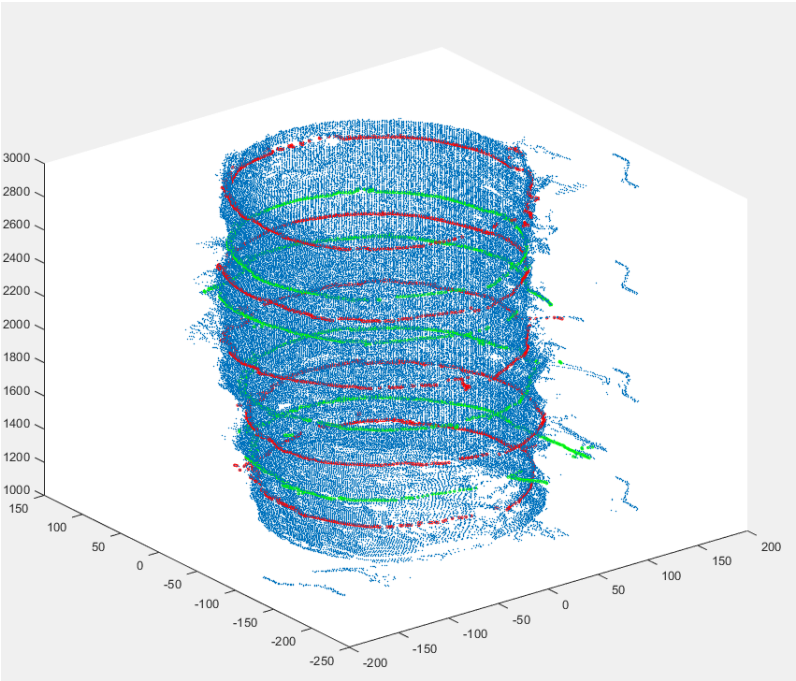

Figure 9. A laser scan of log. Green and red rings mean the beginning and the end of knot clusters.

2.3.3 Knot detection from X-ray tomography

X-ray CT scanning is promising method to non-destructively analysis of the internal structure of wood [26].In the tree trunk there are several zones, performing different functions

and characterized by different properties. It is pith, softwood, hardwood and bark. With X-ray CT scanning it is possible to detect this zones and also internal defects, including knots. Thus, it is possible to detect knots that are not observed on the surface of the log, because either they were broken off during the growth phase, or have not yet sprouted.

Detection of knots with the help of X-ray scanning of log sections. On these sections, the zones of wood, tree rings and knots can clearly be observed. An examples of such images are shown in Fig. 10. Due to the different scanning parameters, the necessary information about wood, such as moisture, age and tree species, can be identified. And after scanning the log completely, a 3-D model can be constructed that reflects both the external and internal structure of the log.

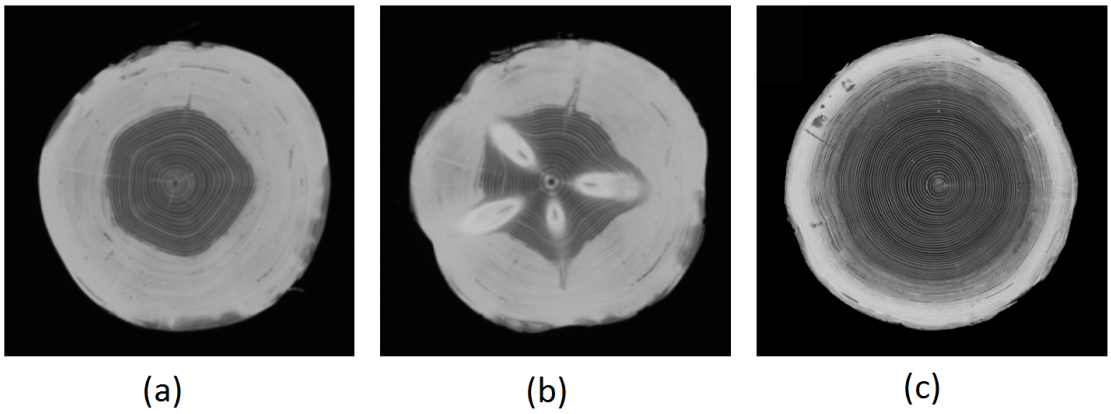

Figure 10. Cross-sectional CT images of: a Scots pine log (a), a whorl of sound knots in a Scots pine log (b) and a Norway spruce log (c). (Modified from [27])

There are several automatic methods, capable of creating 3-D images based on X-ray computed tomography images of log [16]. It is convenient to demonstrate the positions of the knot on these mallets, since their number, size and adherence to the cluster are clearly observed. For the construction of such models it is necessary to find the elements of bitches on cross-sections. Combining the information about the position of the knot with the joint cross-sections, the location of the knot along the trunk of the log can be established [28]. Thus, the exact position of the knot is calculated. Also in the calculation of the position of a knot along a log, lateral X-ray scanning of a log can help. Fig. 11 shows a log model and two types of X-ray scanning.

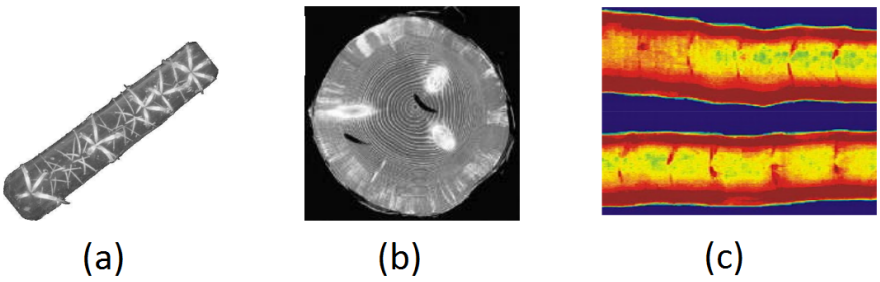

Figure 11. A 3D log model with knots (a), a log cross-section (b) (Modified from [28]) and two scans of a log along (c).

3 DETECTION OF LOG SURFACE DEFECTS

Defects of logs are divided into external and internal. Internal defects are detected during the sawing or X-ray scanning, however, external defects can indicate various damages in the tree trunk. This chapter presents the main types of defects, as well as describes the methods for detecting them from a point cloud surface.

3.1 Types of log surface defects

External defects are associated with a localized log surface rise. The defects of debarked log surface can be divided into branch-related and damage defects. The most serious and common log surface branch-related defects consist of sound knots, unsound knots, overgrown knots and knot clusters. Damage defects include holes and wounds. [24]

3.1.1 Sound knots

A sound knot is a branch stub resulting from either a break or pruning or natural sloughing. The growth of the branch itself leads to a change in the shape of the trunk, thereby forming deformation regions. Thus, the sound knot leaves on the surface a round area without bark, which is significantly higher than the surrounding wood. The bark texture of the new bark over the branch stub is smooth and usually rounded. An example of the sound knot on a surface of a log and on a sawn-off board is shown in Fig. 12. [29]

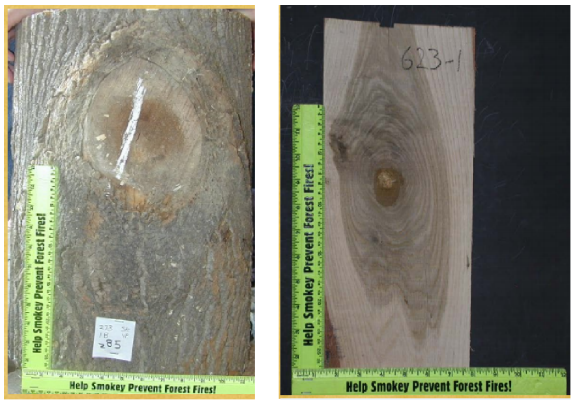

Figure 12. Sound knot on the log surface (a) and the sawn board (b). [30]

3.1.2 Overgrown knots

An overgrown knot is simply the sound knot that has been overgrown or encapsulated within the tree. The knot is completely covered with bark, although there remains a surface rise. Over time, this knot becomes less noticeably on the surface of the tree, becoming an internal defect. The location of the knot on the surface is characterized by at least a single heavy circular ring in the bark texture. An example of an overgrowths caused by knots and manifestation of a bitch in the trunk of a tree is shown in Fig. 13. [29]

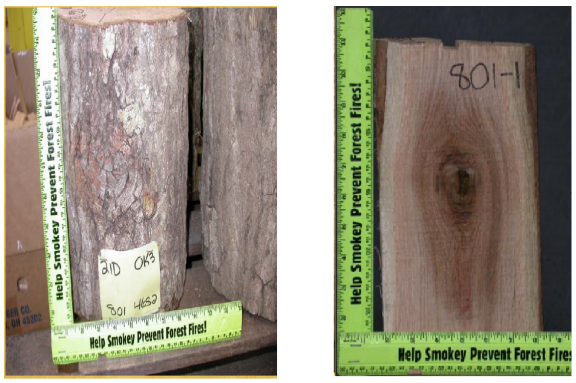

Figure 13. Overgrown knot on the log surface (a) and the sawn board (b). [30]

3.1.3 Unsound knots

If the tree was unable to overgrown the branch stub before decay started or bacterial or viral infection occurs before the tree can completely grow over the branch stub, an unsound knot can occur. Unsound knots have similar overall shape and characteristics as a branch stub with the exception of a rotten area usually in the middle of the defect. The rotten area can be a hole or an exposed piece of the original branch showing signs of decay. An example of such knot is shown in Fig. 14. [29]

3.1.4 Clustered knots

It is common to find two or more knots of the same or different types clustered tightly together. All of the knot defects mentioned above can occur in clusters. Depending on the types of knots clustered, sound knot cluster, overgrown knot cluster, unsound knot cluster

Figure 14. Unsound knot on the log surface (a) and the sawn board (b). [30]

and adventitious knot cluster are singled out. Cluster defects have a greater surface rise than simple knot since the branch defects are growing near and over each other. An example of a cluster in which the bitches are located one under the other is shown in Fig. 15. On this figure is also possible to see the influence of such knots on the inside of the tree. [29]

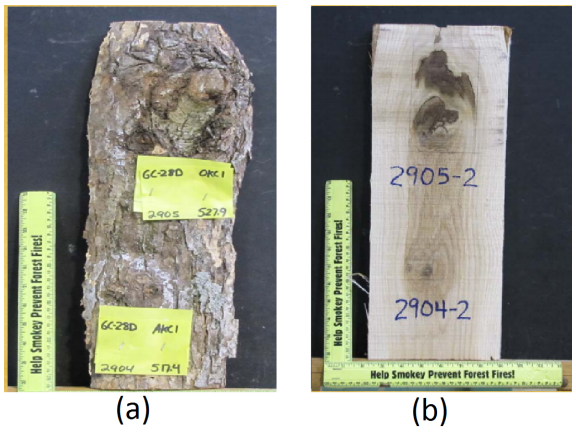

Figure 15. Clustered knot on the log surface (a) and the sawn board (b). [30]

3.1.5 Wounds and holes

A wound is a scar on the bark with no surface rise, usually elongated with a center seam where the edges of the wound grew together. Depending on the severity of the damage, the bark may have a slight depression in the middle of the wound. Wounds may be either new or old. A new wound is essentially a surface injury in which the exposed adjacent

sapwood. An old wound is a similar injury either completely open or only partially healed over. The bark surrounding the wound can appear completely normal. An example of a wound is shown in Fig. 16. [29]

Holes are abrupt depressions into the log surface, which are caused by animals, insects, or decay. In this case, the surface of the tree does not heal in some places, then a place is formed on which the bark does not grow in seasons. The edges of the hole may have surface rise, but usually the surrounding bark can be completely normal with no distortion or other indicator of a defect. The appearance of a hole on the surface of a log is shown in Fig. 17. [29]

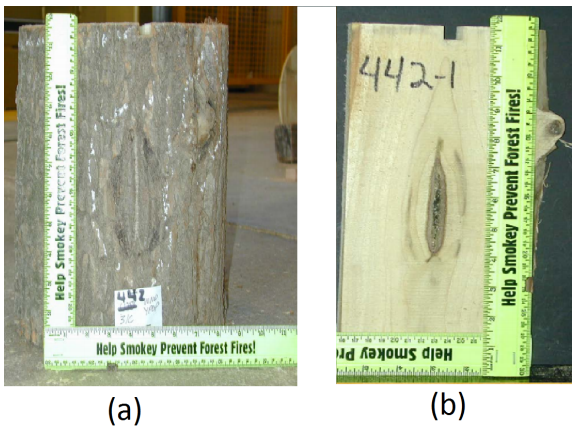

Figure 16. Wound on the log surface (a) and the sawn board (b). [30]

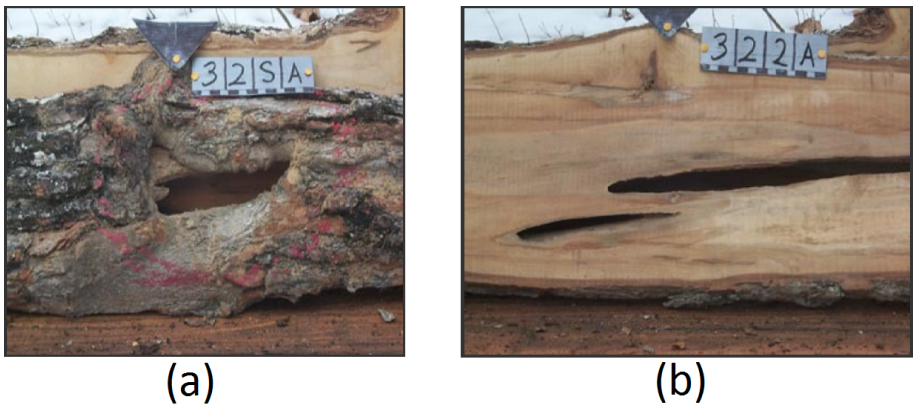

Figure 17. Hole on the log surface (a) and the sawn board (b). [30]

3.2 Method of defects detection

To detect defects on a tree trunk or a log, the data obtained during laser scanning is mainly used. The result of the laser scanning is the point cloud log surface. The laser scanning is prioritized more than the X-ray scan in terms of usability. For example, the laser scanning can be used to scan not yet felled trees [31]. Point cloud is also more useful for working with 3-D models, then than a set of RGB or grayscale images. Obtaining images of the whole surface is not only costly, but also contributes to loss of data about the shape of the log and the structure of the surface. However, the use of the image is applicable, for example, for the detection and classification of damages on sawed boards [23]. These methods are mainly based on the segmentation of the texture of the bark.

Laser scanning with the use of high-quality equipment allows obtaining high resolution models. Fig. 18 shows an example image of a wound on a surface of a tree and its model obtained by laser scanning. Laser scanning equipment collects information about the shape of the external log and the state of the bark using triangulation technology. Main disadvantage for this method is that it only provides external defect information, which might be not enough for lumber processing. [24]

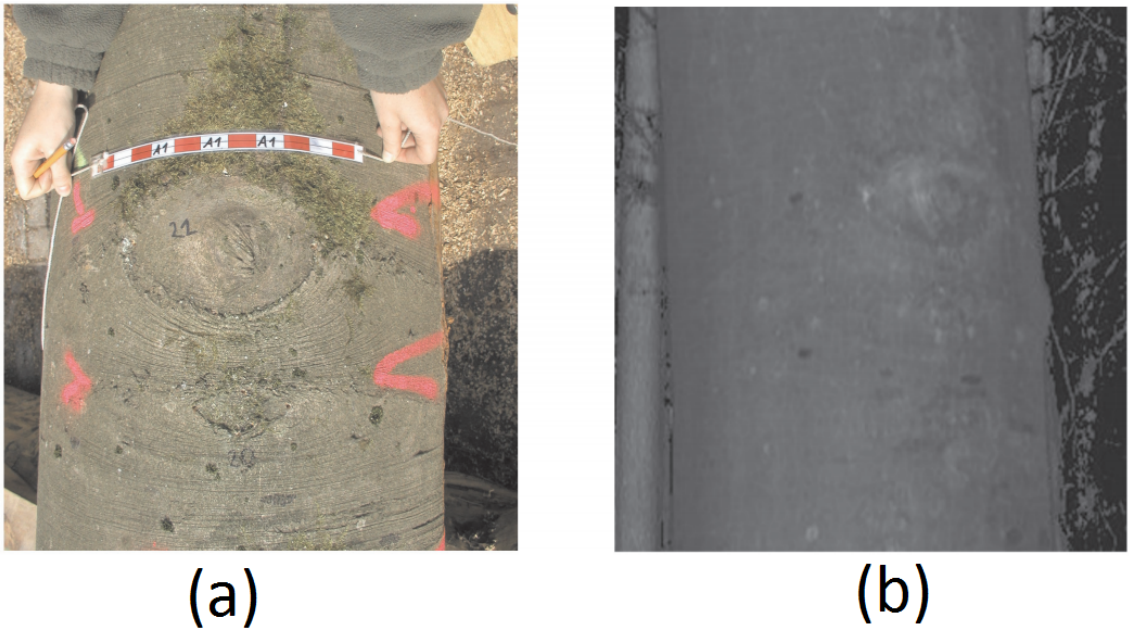

Figure 18. Bark wound on a stem in color (a) and the same wound in the intensity image of the terrestrial laser scanning data (b). [32]

The basic method of detecting log defects is to obtain a 2-D image of the log surface. The

main idea of this method is to define a reference surface that approximates the log surface and define differences between this surfaces. The log, in this case, is unrolled, and its surface is represented as a 3-D image of a practically close to surface or a 2-D image. In the latter case, the intensity of points in the image characterizes the distance from the center of the log to the point. Both representations of the surface of the log are shown in Figs. 19 and 20. The points on the log surface can be then classified by their distance to the reference surface. The reference surface in different methods is defined by cylinders [32] or by circles [24]. Deviations of the bark surface can be detected and visualized and the geometrical properties of bark scars and log defects can be assessed.

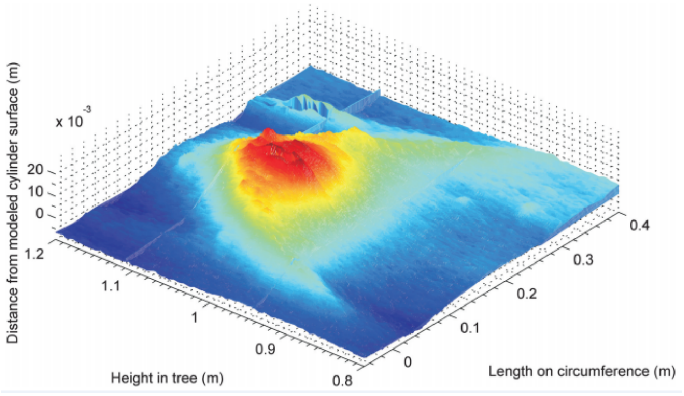

Figure 19. Point cloud interpolation of the unrolled log surface. [32]

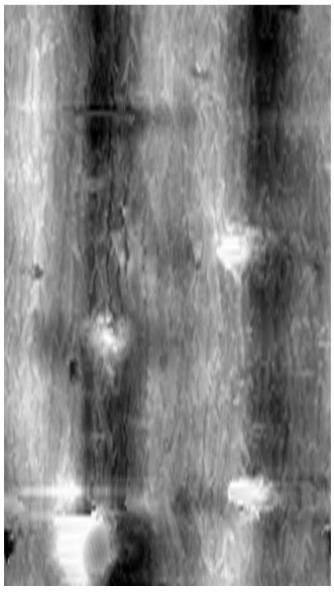

Figure 20. Gray-level range image interpolation of the unrolled log surface. [24]

4 MULTIMODAL MATCHING AND REGISTRATION

In the previous chapters, various ways of obtaining information on the structure of wood at various steps of the sawmilling process were demonstrated. It was also concluded that it is possible to track the wood on the entire sawing process according to the information about knots. This chapter reviews more general multimodal matching methods that could be utilized to track wood.

4.1 Multimodal matching

Multimodal image matching is a method of image co-reduction obtained under different conditions, for example, at different times or using different cameras or sensors. The task of such a matching is reduced to find the optimal transformation between the multimodal image pairs under rotation, scaling and translation transformation conditions. [33] [34]

There are two types of multimodal image matching: global feature-based matching and local feature-based matching. The global object-oriented comparison methods aim at measuring the statistical intensity of the entire image, directly or indirectly. These methods include mutual information [35], Fast Fourier Transform [36] and the correlation matching method [37]. The global functional methods due to dependence on the entire image are susceptible to occlusion, interference and truncation of images. Local feature-based matching images images on the basis of local image features, such as gradient or edge or knot location (for case of lumber tracing). The pairs of features are compared using Euclidean distance or correlation computations. In contrast to global feature-based matching, local feature-based matching methods are more insensitive to affine transformation, occlusion, background clutter and image truncation. [33] [34]

When solving the problem of image comparison, a crucial role is played by a hierarchical analysis of the "primary" features of images-the so-called "characteristic features." Such "characteristics" can be used to compare the current and reference images in a large number of methods, for example, with hierarchical correlation processing, voting methods, or volumetric comparison schemes. In this case, singular points, lines, contours, regions and structures are used as image features. [38]

Fig. 21 shows a simplified multimodal local feature-based image matching process. At the first step, the corners and lines are selected. Then, the selected elements are imageped,

in this example, by using multimodality robust line segment descriptor. [34].

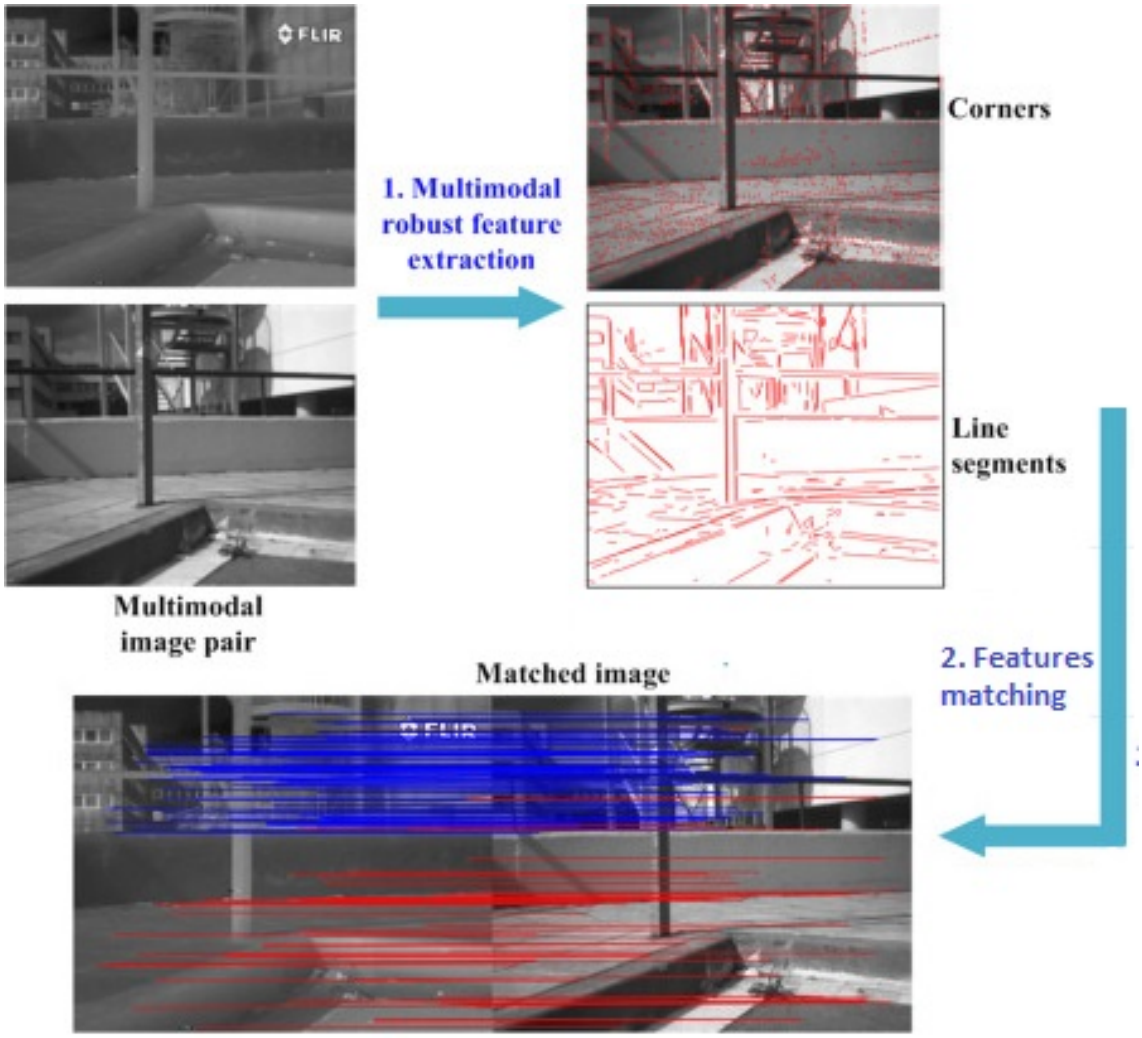

Figure 21. Illustration of multimodal image matching method. (Modified from [34])

4.2 Point cloud matching

Point cloud matching is a special case of the multimodal matching. This method implies the allocation of points on the imageped images and the selection of the corresponding pairs of these points. In this case, the selected points should carry information about the structure and position of the objects on the images, like corners [39] and edges [40]. Recently, the method has proven itself to solve the problem of comparison of points from the 3-D scanning of an object. Matching of point clouds is challenging in that there is usually an enormous number of 3-D points and the coordinate system can vary in terms of trans-

lation, 3-D-rotation and scale. Additional complexity is caused by noise and occlusions. This method is extremely useful when points are known only from their coordinates, and information about the structure, such as color, intensity or texture, is missing. [41]

One of the most widely used rigid registration algorithms is the iterative closest point (ICP) [42]. ICP is an algorithm employed to minimize the difference between two clouds of points. ICP is often used to reconstruct 2-D or 3-D surfaces from different scans, to localize robots and achieve optimal path planning. The algorithm is conceptually simple and often used in real time. It repeatedly applies the transformations (displacement, rotation) necessary to minimize the distance between the points of two raw scans. The algorithm implies a bundle of points by the nearest neighbor criterion to estimate the transformation parameters using the root mean square (RMS) value function and transform points using estimated parameters. The algorithm can be repeated many times, and the points can be connected each time. [43]

4.3 Multimodal registration

Multimodal image registration is aimed at evaluating spatial correspondences between pairs of images from different visualization methods. With the general registration of images, these correspondences are calculate by finding a spatial transformation that makes the transformed original image the most similar to the fixed target image. It is a challenging problem due to the high variability of object appearance under different imaging modalities. The task of aligning two images is cast as an optimization problem: a common approach to registration is to deform one of the images so as to maximize its similarity to the other image while maintaining a “smoothness” in the estimated deformation field. Most of the similarity measures can be classified into two categories: feature-based and intensity-based [44]. For multimodal imaging similarity of images has to be high, if the images are close to identical, which allows using simple measurements of similarity of the image, such as the sum of squared intensity differences (SSD) between pairs of images. Evaluation of the similarity of images between modalities is much more difficult, since the appearance of the image can vary widely, for example, because of the different basic principles of physical visualization. Consequently, more complex measures of multimodal similarity are required. In addition, the results of image registration are controlled both by the chosen similarity measure and by the deformation model chosen. Therefore, especially for multimodal image registration, where the estimation of image similarity becomes difficult, considering the importance of the similarity method in conjunction with the deformation model. [45]

5 PROPOSED METHOD FOR KNOT DETECTION

To determine the position of the knots in logs from laser point cloud of log surface, the detail information about an external defects corresponding to rises or depressions on log surface is needed to be computed. The proposed method to detect knot positions from laser scan data consists of the following processing steps:

1. Fit 2-D circles to each log cross-sections.
2. Reconstruct surface of the log by extracting differences between circles and the log.
3. Locate the knot positions characterized by a significant surface rises.

5.1 Circle fitting method

The laser scanning data are represented as a set of points in 3-D space. An examples of point cloud projections of 3-D log data are shown in Figs. 22 and 23. These images represent the same log at different scales of axes.

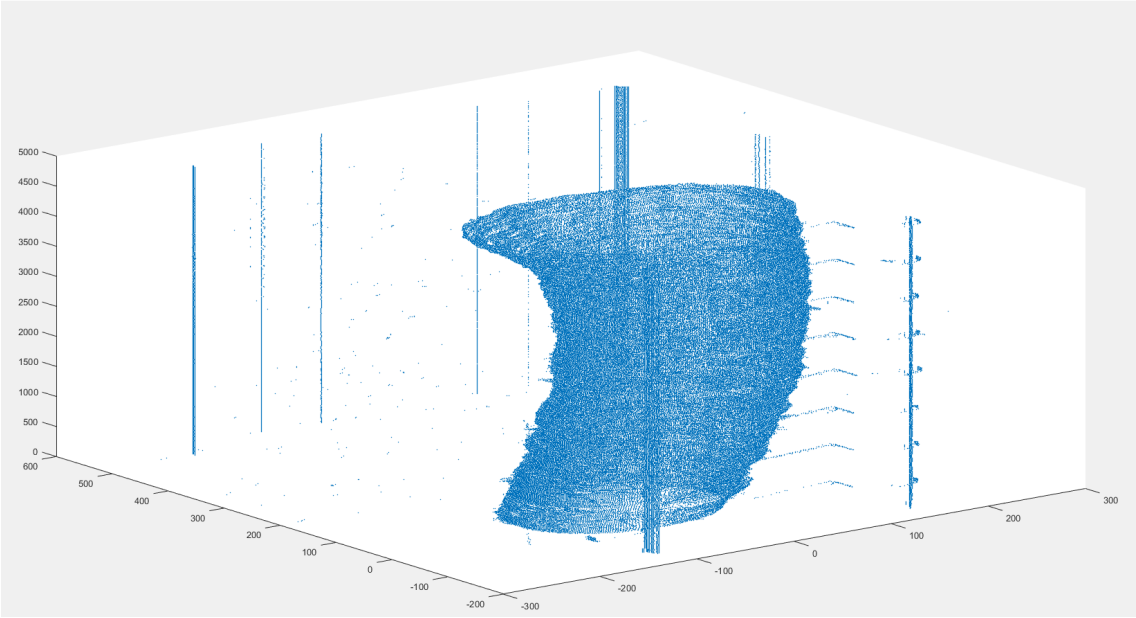

Figure 22. Example of the point cloud image.

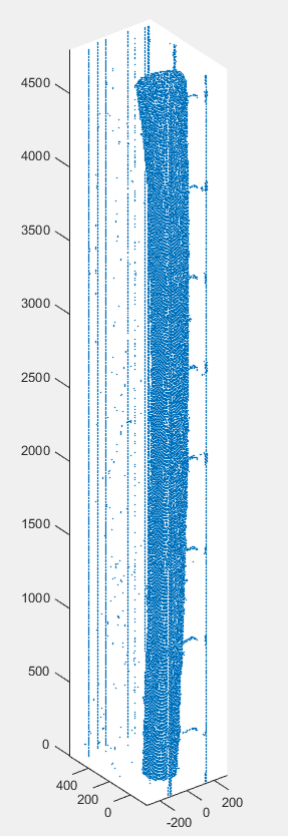

Figure 23. Example of the original data with real proportions.

Since logs have a deformed cylindrical shape it is convenient to approximate them with a cylinder. However, typically logs have noticeable bends and expansions which do not allow the data to be approximated by a single model. To this end, it was decided to approximate each cross-section of the log. An example of one cross-section is shown in Fig. 23. It can be seen that the data contains a significant number of outliers. In this regard, for the fitting of the circle, it was decided to use the RANSAC (Random Sample Consensus) fitting method [46] with subsequent post-processing of the data.

5.1.1 Random sample consensus

RANSAC is a stable method for estimating the parameters of a model based on random samples. RANSAC work well with source data with large number of noise and outliers. The essence of the algorithm is the pick of random points from a common data array. Based on the selected points, parameters of fitting model, which is usually called the hypothesis, are calculated. By using the estimation function and the threshold value, the correspondence to this hypothesis is checked for every point of data set. The number of

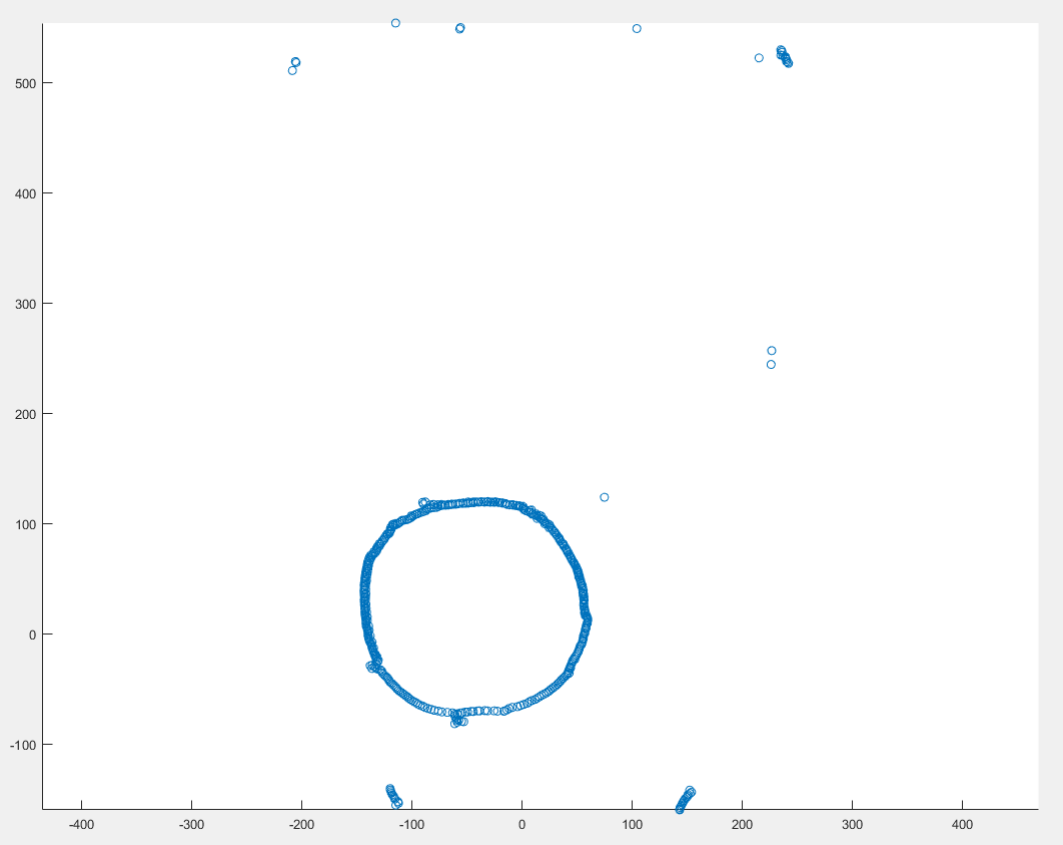

Figure 24. Example of log cross-section data.

points that satisfy the model is counted, and if their number is greater than some threshold value, this hypothesis is considered as suitable for the data. Then the algorithm is repeated with another set of random selected points, and the best model obtained from them is chosen. The basic algorithm is shown in Algorithm 1. The advantage of the RANSAC method when working with noisy data is shown in Fig. 25. [46]

The advantage of the RANSAC algorithm is its ability to provide a reliable estimate of the model parameters, that is, it is possible to evaluate the model parameters with high accuracy, even if a significant number of emissions exists in the initial data set. One of the drawbacks of the RANSAC method is the absence of an upper time limit for calculating the model parameters. If the maximum number of iterations is used as a certain time boundary, the resulting solution may not be optimal, and there is a very small probability that no model matches the original data. The exact model can be defined with some probability, which becomes larger the more iterations that are used. Another drawback of the RANSAC method is that it is necessary to set a specific threshold for the algorithm to execute. Finally, using RANSAC, only one model can be defined for a particular data set. As with any approach intended for one model, the following problem exists: when there

Algorithm 1 RANSAC

INPUT: a set of observed data points X
a model that can be fitted to data points P
minimum number of data points required to fit the model n
maximum number of iterations allowed in the algorithm k
threshold value to determine when a data point fits a model t
number of close data points required to assert that a model fits well to data d
OUTPUT: model parameters which best fit the data

```
1:  while number of occurred iterations is less than k do
2:      randomly select n points from X dataset
3:      calculate model P parameters fitted to selected points
4:      for every point in X do
5:          point fits calculated model with an error smaller than t
6:          if point fits model then
7:              increase number of inliers
8:          end if
9:      end for
10:     if the number of inliers is more than d then
11:         if model with new parameter fit better than previous models then
12:             accept this model as the best fitted model
13:         end if
14:     end if
15:     increment iterations
16: end while
```

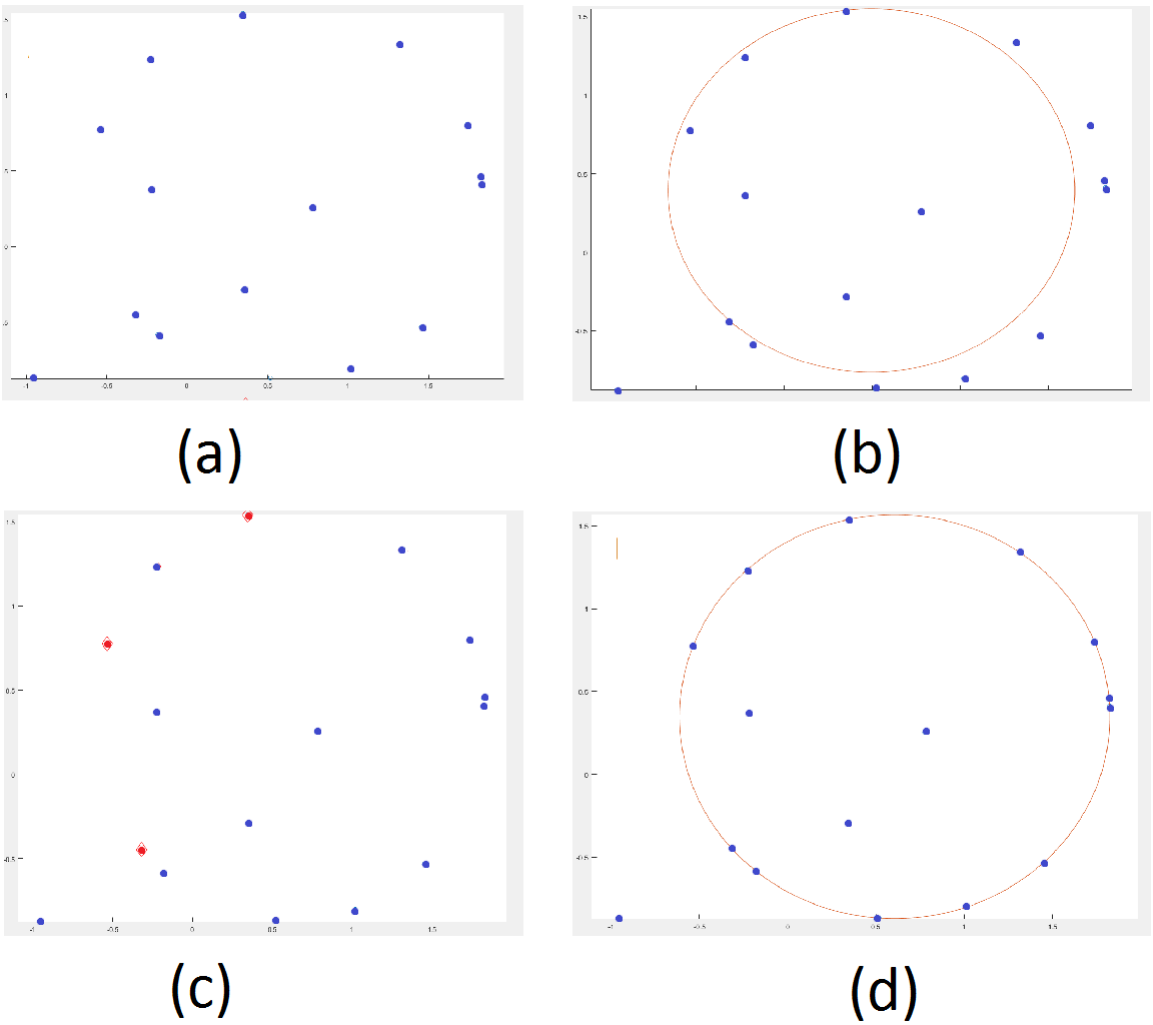

Figure 25. Fitting an circle to a noisy point sequence: The figure shows data with multiple emissions (a); The circle that is fitted to all data (b); The effect of emissions on the model is evident; Random points are selected from data set (c).These are highlighted in red; The corresponding circle is shown on last image (d); The model fully fit to the initial data.

are two (or more) models in the source data, RANSAC can not find any.

In this work, the method was used to fit each cross-section of a scanned log using a circle [47]. The approximation by the ellipse turned out to be unacceptable since although a small number of emissions was observed, it often took the outliers points as the base points of the log. Fig. 26 shows how, for the same set of points, the approximation by an ellipse took the ejection at the right of the log cross-section for correct points, because of which a strong deformation on the image of stem surface can be missed. The obtained circle models are used to remove the outliers points and noisy layers gained from scanning.

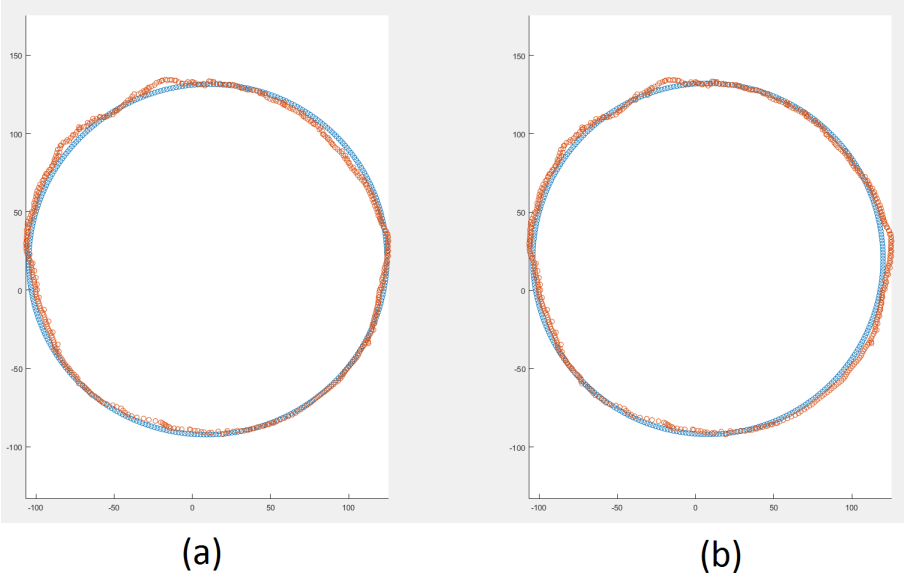

Figure 26. Comparison of two methods of approximation: by ellipse (a) and circle (b).

5.1.2 Data preprocessing

Inaccuracies in scanning process and shaking of log during scanning lead to the appearance of emissions and data loss. An examples of defective cross-sections are given in Fig. 27. To remove such noise, the circles obtained from the RANSAC method is used. The estimated center and radius of the section of the log were calculated. The distances from each point of the section to the center were calculated, and if this distance was very different from the expected radius, then it was estimated as an ejection. Sections were also deleted which fitting circles have significantly different centers and radii from mean values of all cross-sections.

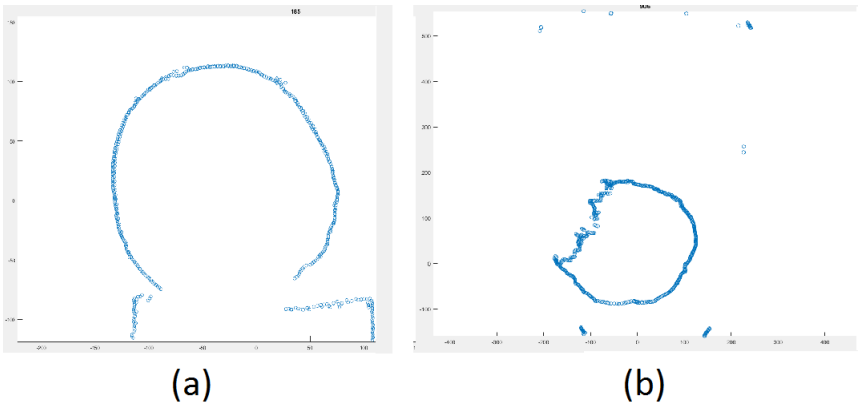

Figure 27. Example of problem cross-sections: data loss with ouliers (a) and noisy layer (b).

At the end of this stage, only the points that can be perceived as the true points of the log remain, with distortions caused by the defects of the surface or remnants of the bark. The result of this filtering is shown in Fig. 28.

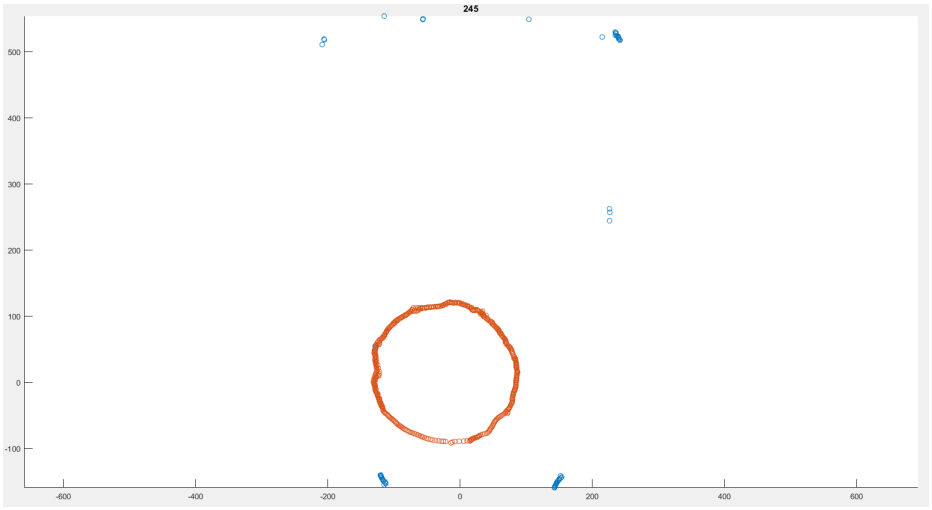

Figure 28. Filtering example: noise from original data (blue) and filtered data (orange).

5.2 Surface reconstruction

To determine the position of the knot, a image image of the tree stem surface is constructed by using data from 3-D point cloud. This image is useful to observe height changes of the surface: protrusions or concavities. Often, the protrusions on the trunk are the consequences of knot growth. The first step in creating a surface image is to move points to a cylindrical coordinate system [31].

A cylindrical coordinate system is a 3-D coordinate system that specifies point positions by the distance from a chosen reference axis, the direction from the axis relative to a chosen reference direction and the distance from a chosen reference plane perpendicular to the axis. The cylindrical coordinate system can be considered as an extension of the polar coordinates in 3-D. The position of the point specifies by the coordinate of the height of the point, the distance of the point from the center and the angle of inclination of the point from some selected axis in the cross-section plane.The example of transformed 3-D point cloud surface in the new coordinate system is shown in Fig. 29.

Then, a 2-D image of the surface of the log is constructed. A surface image is created in which the coordinates of the point denote its height and angle, and the intensity is

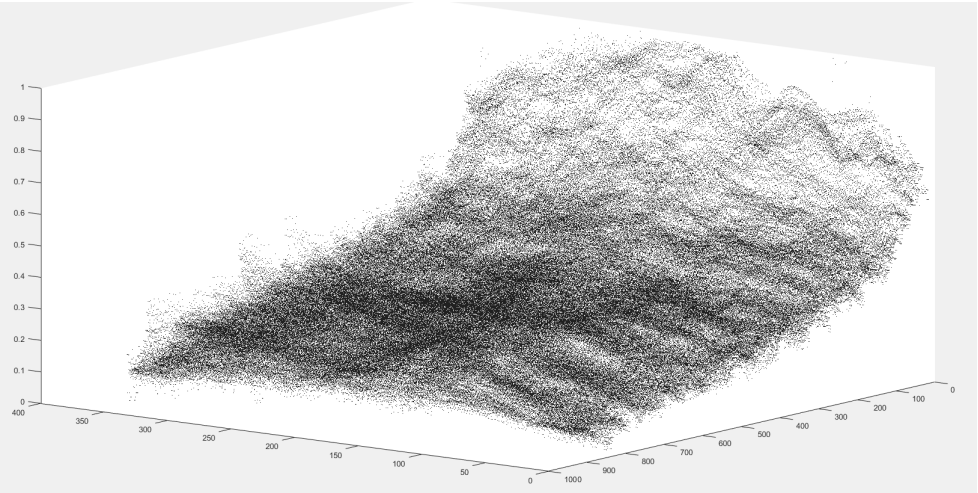

Figure 29. Transformed 3-D point cloud in the cylindrical coordinate system.

indicated by the distance from the center of the log. However, in most cases log cross-sections have different radii, which can lead to a certain definition of the geometric shape of the log characteristics. For example, in Fig. 30, the log is widened from above, so the points above have more distances to center. In this case it is hard to accurately detect stem feature of the full log. To avoid this, it is necessary to calculate the distance between points along the side of the virtual cylinder representing the tree stem. Thus, it is possible to estimate the surface invariantly to the radius of the section.

Using the parameters of the circles previously calculated, it is possible to compute the radial distance, which corresponds to the difference between the distances from the center of the section to the point and the radius of the circle. Fig. 31 presents an example for the numerical simulation of the surface for one of the log. Specific log features on the tree stem surface can be visually detected due to the chosen jet-color image: scars and branched knots are shown in green-yellow-red spectrum.

5.3 Knot detection

Having a display of the unevenness of the trunk, the alleged position of the knots can be determined. To do this, select the field with the perturbation of the surface. However, since the calculation of the distances occurred independently for each cross section, a spread is possible between neighboring points of the resulting image. To prevent possible data loss, the image is filtered with the bandpass filter and thresholded.

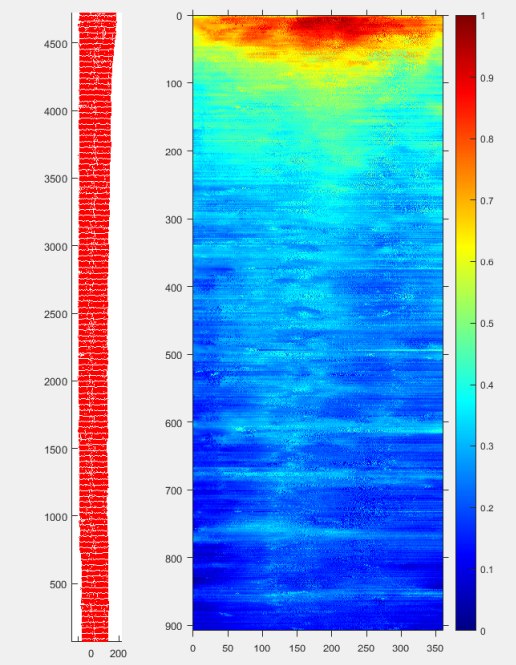

Figure 30. The log (left) and its corresponding surface image (right). The distance is calculated between point and center of the log.

5.3.1 Bandpass filtering

A bandpass filter [48] attenuates very low and very high frequencies, but retains a middle range band of frequencies. Bandpass filtering can be used to enhance edges (suppressing low frequencies) while reducing the noise at the same time (attenuating high frequencies). The filter function is obtained of a bandpass by multiplying the filter functions of a low pass and of a high pass in the frequency domain, where the cut-off frequency of the low pass is higher than that of the high pass. Therefore in theory, one can derive a bandpass filter function if the low pass filter function is available. Bandpass filtering is attractive but there is always a trade-off between blurring and noise: low pass reduces noise but accentuates blurring, high pass reduces blurring but accentuates noise.

In this work the Butterworth bandpass (BP) filter [49] is used for smoothing image and leaving out noise. This filter can be derived mathematically by multiplying the transfer functions of a a low passs (LP) and high pass (HP) filter. The low pass filter has the higher cut off frequency. The main formulas used for filtration are as follow:

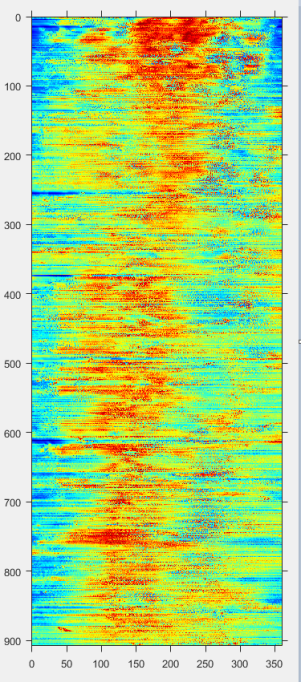

Figure 31. Surface image.The distance is calculated between point and approximated circle.

$$H_{LP}(u,v) = \frac{1}{1 + [D(u,v)/D_L]^2 n} \tag{1}$$

$$H_{HP}(u,v) = 1 - \frac{1}{1 + [D(u,v)/D_H]^2 n} \tag{2}$$

$$H_{BP}(u,v) = H_{LP}(u,v) * H_{HP}(u,v) \tag{3}$$

where D_L and D_H are the cut frequencies of the low and high pass filters respectively; n is the order of the filter and $D(u,v)$ is the distance from the origin. The Butterworth filter has a "smooth" transfer function without any discontinuity or clear cut off frequency. The range of frequencies that the filter allows is largely dependent on the order of the filter. In the selection of n there has to be a compromise between the demands of the frequency domain (sharp cutoff) and the spatial domain (rapid decay). The result of Butterworth bandpass filtering of surface image shown in Fig. 32.

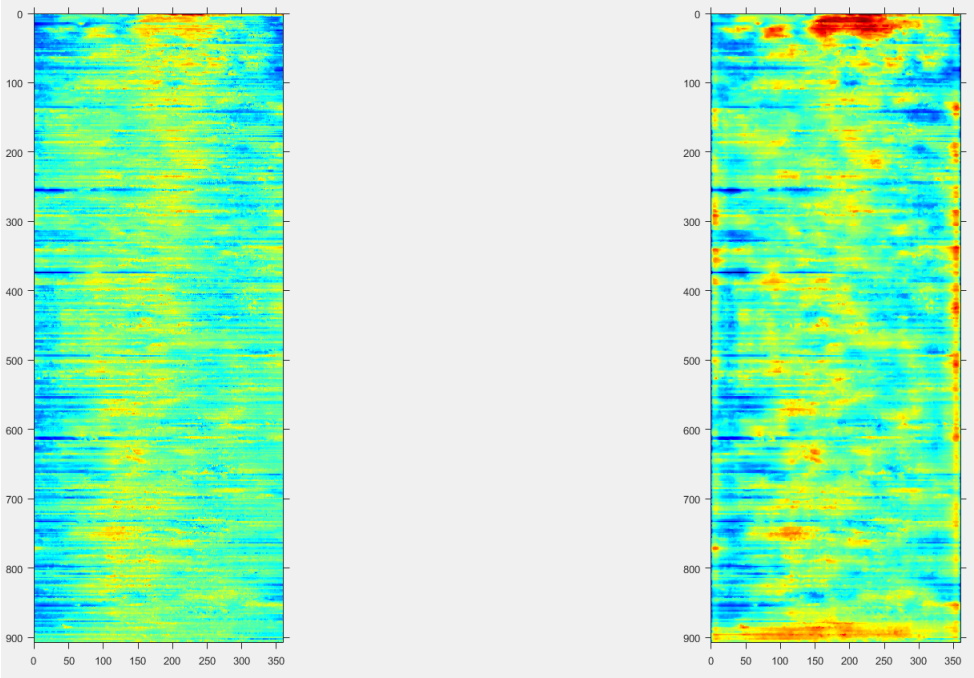

Figure 32. The surface image (left) and bandpass filtered image (right).

5.3.2 Thresholding

To detect bitches on the image of the surface of a log, the areas of noticeable changes in the height of the surface are determined. To do this, the levels of heights on this image are distinguished, which can be performed using the threshold process. Taking into account the structure of the provided logs, three areas were identified: area below, above, or on a par with the basic surface. To select these areas, the Otsu's thresholding method was applied.

To determine the first type of surface rises, the Otsu's thresholding method [50] was used. This method is mainly used for reduction of a gray-level image to a binary image. The Otsu's method has shown its effectiveness for working with images that can be divided into two classes. The algorithm calculates the optimum threshold separating the classes so that their intra-class variance is minimal, or equivalently, so that their inter-class variance is maximal. The detailed description of the algorithm is given in Algorithm 2.

In the other way,the Otsu's method is extended to support multiple levels instead of only two levels [51] [52]. The multilevel Otsu's thresholding method selects several threshold values to classify the pixels of image into several classes, thus it can handle complicated images. multilevel Otsu's thresholding method was applied to search for three level of

Algorithm 2 Otsu's method

INPUT: grayscale image $I(x, y)$
OUTPUT: threshold value for binary image

1: compute histogram and probabilities $p(l)$ of each intensity level l of image I
2: set up initial class probabilities $\omega_i(0)$ and mean $\mu_i(0)$ for two classes
3: **for** each possible intensity value t = 1...maximum intensity **do**
4: calculate $\omega_i(t)$ and $\mu_i(t)$
5: compute inter-class variance $\sigma_b^2(t)$
6: **end for**
7: chose threshold value corresponds to the maximum $\sigma_b^2(t)$

the surface image, and the upper threshold was used to determine the highest level on the image. An example of highlight areas on surface image is shown in Fig. 33

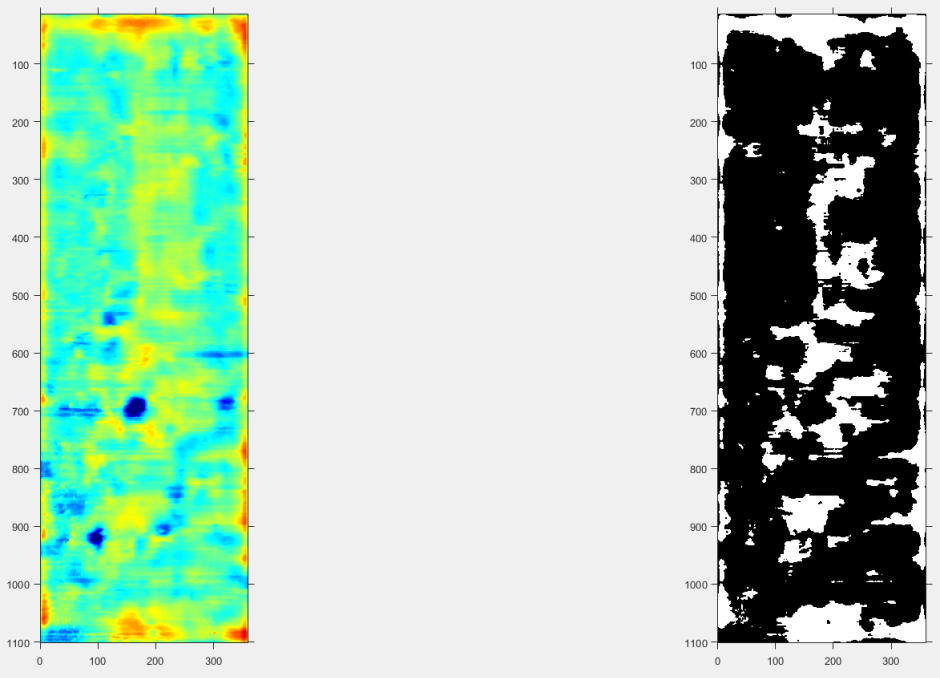

Figure 33. An example of a surface (left) and its corresponding binary image with highlighted the highest area (right).

The use of areas obtained by the method shows even slight elevations of the surface, which helps to find poorly expressed knots positions. However, in this way it is impossible to detect places with the local significant surface rises. And it is in such places that the knots are supposed to be located. To detect such zones, a simple threshold method was used, which reserved only areas with the maximum height of the surface. An example of the

resulting image is shown in Fig. 34

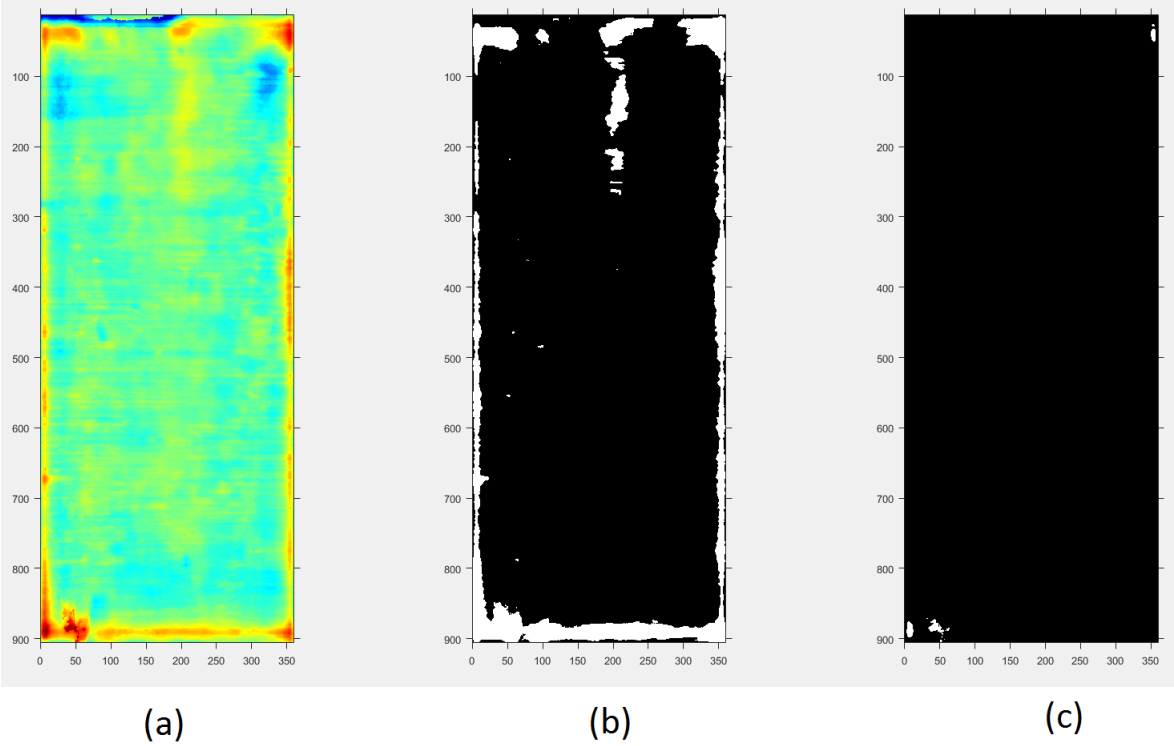

Figure 34. An example of filtered color image of the surface (a), its binary surface images with highlighted the highest area (b) and local significant surface raise (c).

5.3.3 Knots localization

As a result of the previous operations, the image with isolated sections with an elevated height of the log surface was obtained. From this image, the possible locations of knots can localized. For this, the assumption is made that the size of the knot is not large compared to other defects in the log's outrigger. Thus, the problem is reduced to the detection of regions of altitude.

Taking into account the fact that the knots are fairly compact, it is necessary to highlight the peaks in the changes in the heights of small size. In order to obtain a knot position, two types of change were sought on the resulting image. The first is a local insignificant increase in surface elevation, and the second is the peaks of significant elevations of the surface. For these purpose contours of points of height were constructed and regions of size aren't exceeding a 0.1 m in diameter were found among the obtained regions. An

example of a surface and its corresponding binary images is shown in the Fig. 35. By using this image, it became possible to calculate the number of knots on the surface of a log, as well as obtain the coordinates of their locations.

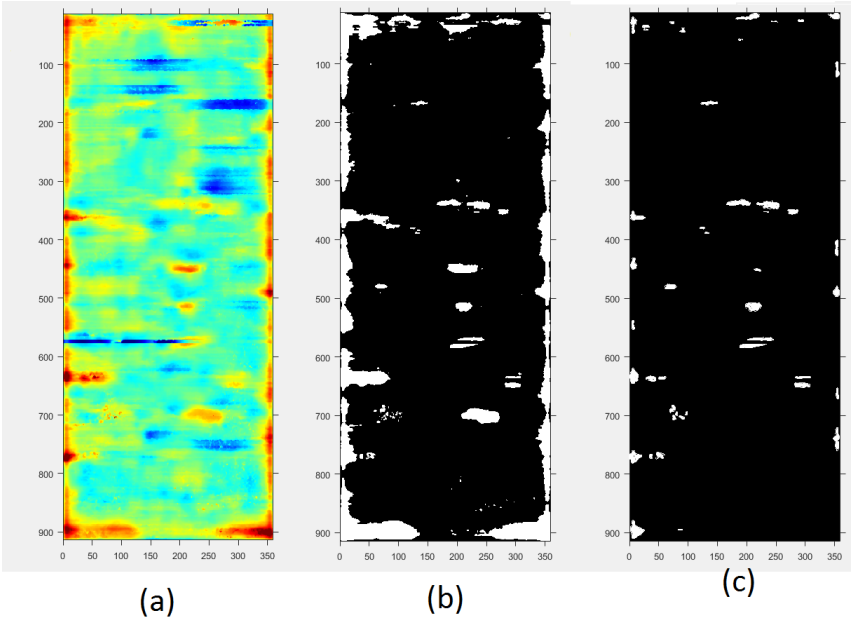

Figure 35. An example of filtered color image of the surface (a), its binary surface image (b) and selected regions of knot position (c).

6 EXPERIMENTS

6.1 Data

Input data are presented as cloud points obtained after laser scanning the log. The 3-D log surface data consist of a collection of 3-D range data points grouped as circular-shaped cross sections from the scanner. Because of the complexity of scanning, there is a loss of points on the bottom side of the log. This is related with the lying position of the log on the conveyor. An example of input data and a cross-section of the log with distinctly shortage of points on the bottom base of the log are shown in Fig. 36.

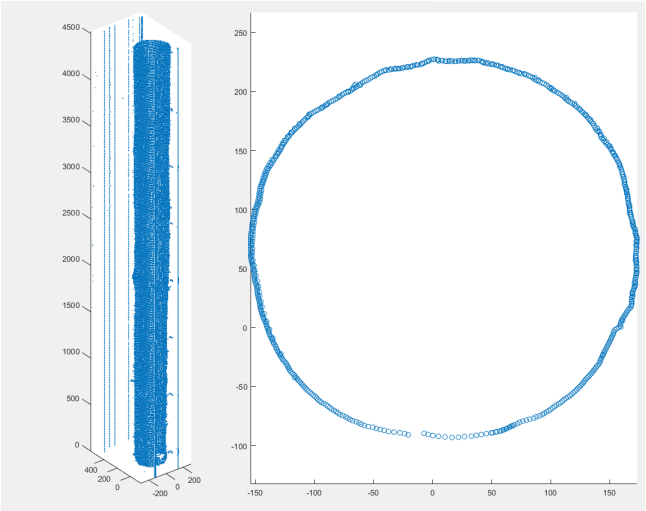

Figure 36. An example of input data (a) and cross-section of the log (b).

The work was carried out with 50 different pine logs, each of which was scanned four times with same parameters, so the total data size is 200 point clouds of logs. The average length of the log is five meters, and the number of cross-sections is in the range of 900-1100. The distance between the cross-sections is 0.0052 m. The number of points on each cross-section is varied from 50 to 1000, the average number of points is 750.

Also, information on the position of clusters of knots obtained by using X-ray scanning was attached to the data. Data contains information about clusters inside a log that can not be observed on the surface. Therefore, this X-ray data does not provide complete information about the positions of knots and can be used with an eye to it. Also data only describe the sections where the knot clusters are located, without details of their position

on the log surface, or the number of knots in cluster. An example of such data is shown in Fig. 37.

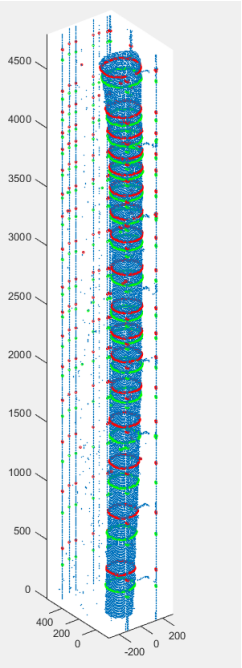

Figure 37. An example of a point cloud of a log with selected sections containing knot clusters. Green marks the beginning of such a section and red marks its ending.

6.2 Implementation

The work was carried out using multi-paradigm numerical computing environment MATLAB (matrix laboratory) version 9.2.0.538062 (R2017a). Cirle fitting was computed by RANSAC method, smoothing and blurring reductions were implemented by Butterworth bandpass filter. Parameters of this methods are shown in Table 1.

Table 1. Percent of correctly observed clusters per log

RANSAC maximum interaction number	1000
RANSAC number of random point chose at every interection	3
RANSAC threshold value	5
RANSAC number of close data points in good fitted model	50
Butterworth bandpass filter low pass frequency	10
Butterworth bandpass filter high pass frequency	50

6.3 Results

The efficiency of the algorithm for finding knots was evaluated by comparing the position of the found knots with the information obtained by X-ray scanning. To do this, it was checked that in the clusters area specified by the X-ray scan data there is an assumed location of the knot. Fig. 38 shows the position of the found knots with the selected areas containing clusters. The full information about knots and knot clusters are shown in Table 2. This data was used for calculating number of clusters with at least one detected knot in their areas and number of detected knot, which are lying inside cluster area.

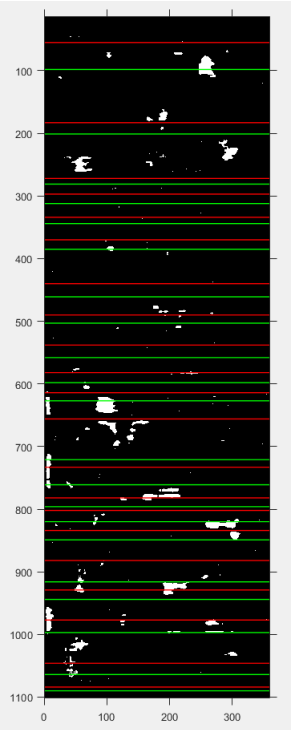

Figure 38. An example of an surface image of with selected sections containing knot clusters. Green marks the beginning of such a region, red - its ending. White borders denote knots

6.3.1 Number of correctly observed clusters

The number of correctly observed clusters makes it possible to estimate how accurately this method can detect a cluster. In this case, the cluster is considered confirmed if at least one knot is found in it. Such an assumption was made on the following pristine. The information about the areas of the cluster does not give full confidence that all the knots of the cluster will be able to observe the log's damage. The data obtained with the X-ray

Table 2. The numbers of knots and clusters.

Log	Clusters	Knots	Log	Clusters	Knots
1	11	39	26	10	43
2	10	39	27	10	44
3	17	56	28	1	38
4	20	40	29	9	64
5	10	46	30	9	45
6	16	34	31	18	33
7	13	41	32	6	21
8	14	59	33	13	43
9	16	47	34	3	43
10	8	69	35	8	24
11	13	53	36	11	30
12	14	51	37	13	60
13	15	3	38	17	59
14	10	60	39	14	23
15	14	42	40	11	34
16	12	27	41	13	55
17	13	40	42	15	50
18	7	44	43	13	48
19	19	67	44	20	45
20	11	31	45	14	46
21	14	79	46	12	20
22	8	47	47	22	22
23	14	67	48	13	42
24	13	14	49	8	53
25	13	63	50	16	46

scan contain information about knots inside the tree, which laser scanning simply can not detect. For each log, the ratio of the number of clusters detected by knots to the total number of clusters detected by X-ray scanning was calculated. The average percentage was 71.1%, which, given the difficulties with finding a cluster, is a positive result.

The Table 3 shows the percentages of cluster detection and, in accordance with it, the graph shown in Fig. 39 is constructed. The Fig. 40 shows the dependence of the number of logs on the percentage of correctly detected clusters. The graphic shows that the number of logs with a high percentage of identified clusters (over 80%) is rather small and at the same time at least 20% of clusters cant be observed at every log. However, this result is acceptable, since, as was said earlier, there is no complete certainty that in the zone designated as the cluster location area, one can actually detect its elements.

Table 3. Percent of correctly observed clusters for each log: 71.1% on the average.

Log number	1	2	3	4	5	6	7	8	9	10
%	86	88.6	74.7	74.7	97	73.8	83.1	84.1	79.7	92.6
Log number	11	12	13	14	15	16	17	18	19	20
%	80.9	84.1	75.6	96.7	82.3	83.2	70.5	91.2	88.8	61.1
Log number	21	22	23	24	25	26	27	28	29	30
%	82.3	89.5	89.5	43.9	82.7	74.5	82	75.6	93.6	82.5
Log number	31	32	33	34	35	36	37	38	39	40
%	47.6	22.8	46.0	39.5	29.7	54.8	79	83	32.3	50.3
Log number	41	42	43	44	45	46	47	48	49	50
%	62.1	56.9	53.9	73.4	73.9	54.2	50.6	66.4	62	73.2

6.3.2 The number of knots found within the supposed areas of clusters

Another parameter for estimating the accuracy of the knot detection method is the ratio of knots found in the area of the cluster to the total number of knots, detected on the log surface. Since the conclusion about the inherent knot was made only on the basis of a change in the height of the log's surface, that is, the probability of a false definition of a knot. This is possible in areas in which surface elevation is caused by either log defects or errors in scanning. Thus, this parameter allows to estimate the reliability of the detected knots. It should also be noted that, as it was said earlier, not always in the area of the supposed existence of a cluster, a knot could be found.

Data on the percentage of knots found in the zone of the cluster are shown in the Table 4) and in Fig. 41. They show that the average percentage of detection of a knot in the cluster cluster is approximately 43.4%. This result is also positive, because, as it was told earlier, the X-ray scan data do not give a complete probability that even a single knot will be detected in the cluster area. The Figs. 41 shows that the parameter takes minimum values at logs 32 and 34. This may be due to the fact that, according to the Table 2, these logs have the smallest number of clusters, and therefore the chance to detect a knot in the cluster area is less. The Fig. 42 illustrates that significant number of logs have (60%) have more than half of the knots outside the cluster area. Which is true, given that the data of the X-ray scan only describe clusters of knots and do not give a complete idea of the number of knots outside these clusters.

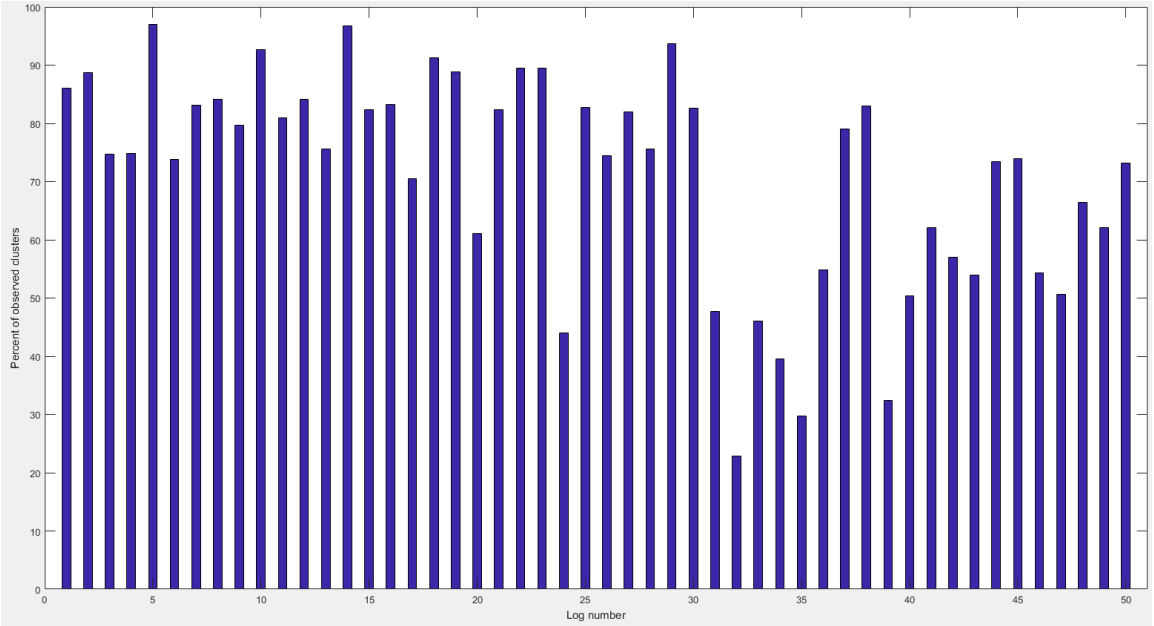

Figure 39. The probability of cluster detection for each log.

6.3.3 Dependence on the threshold value

In addition, an experiment was performed to determine the effect of the threshold value when determining the rise of the surface by the number of knots detected in the cluster of knots. To do this, instead of applying the Otsu's thresholding method that calculated the threshold value for each log individually, a single threshold value was used for all the logs. The result of the experiment is shown in Fig. 43.

It shows that with increasing threshold value, there is an increase in the detected clusters simultaneously with a decrease in the number of bitches found in these clusters. This indicates that most of the found knots were found inappropriately. Then approximately by 48% the number of areas of clusters with a bough begins to fall, and the number of knots in clusters on the contrary grows. Thus, the knots began to be in the area of clusters, and the false detection of clusters due to incorrectly found knots, decreased. It is worthwhile to clarify that the average threshold value for all logs obtained by the Otsu's method is 0.5028, which indicates good thresholding of the image by this method.

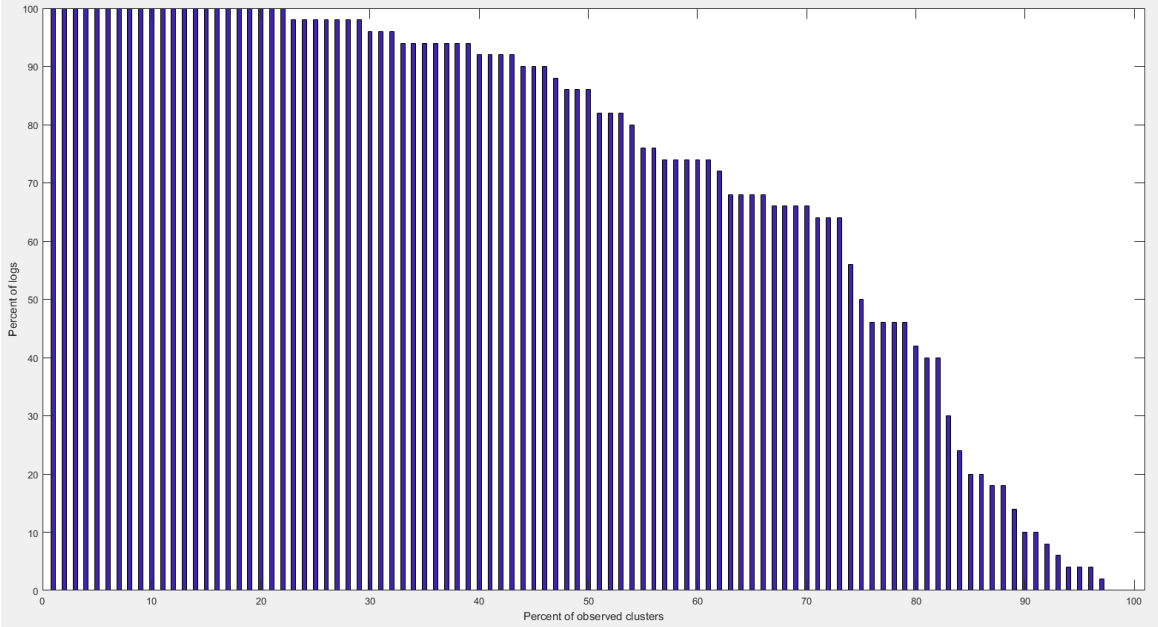

Figure 40. The number of log with each probability.

Table 4. Percent of detected knots in the knot cluster area for each log: 43.4% on the average.

Log number	1	2	3	4	5	6	7	8	9	10
%	58.8	48.5	46.6	68.2	55	64.9	70.7	50.7	56.2	30.8
Log number	11	12	13	14	15	16	17	18	19	20
%	40.4	56.4	60.6	45	65.3	68.6	54.8	38.6	55.2	41.3
Log number	21	22	23	24	25	26	27	28	29	30
%	32.3	42.1	47.5	54.9	37.6	40.6	52.7	38.4	44.1	36.6
Log number	31	32	33	34	35	36	37	38	39	40
%	37.8	4.8	21.2	4.4	11.3	30.5	36.8	50.2	47.6	23.4
Log number	41	42	43	44	45	46	47	48	49	50
%	30.9	26.4	24.9	55.3	38.9	60.2	59.6	37.5	13.5	50.8

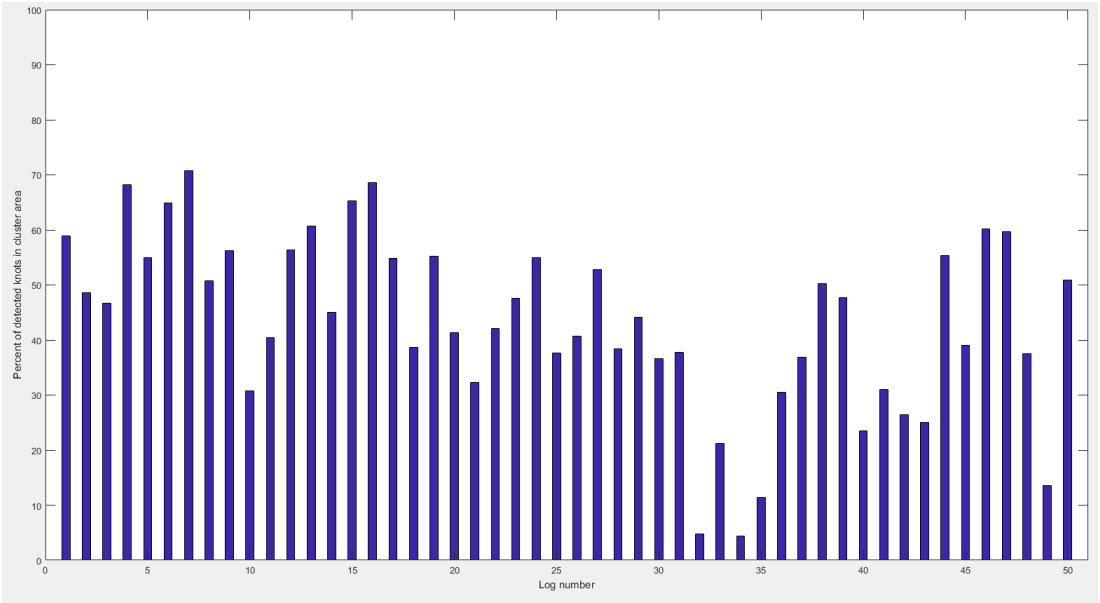

Figure 41. The probability of detecting a knot in the cluster area

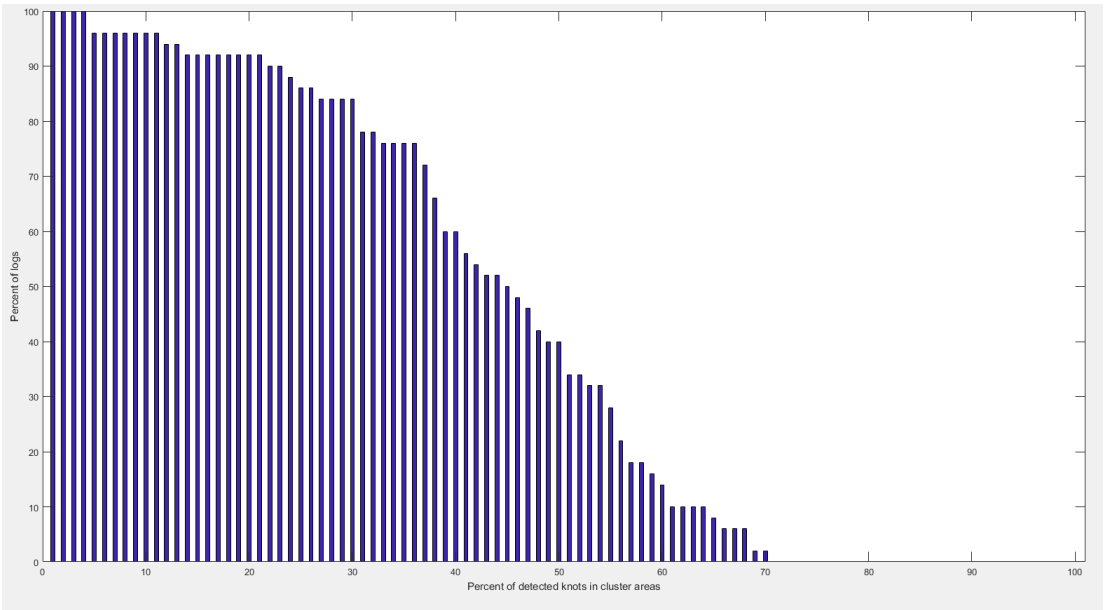

Figure 42. The number of log with each probability

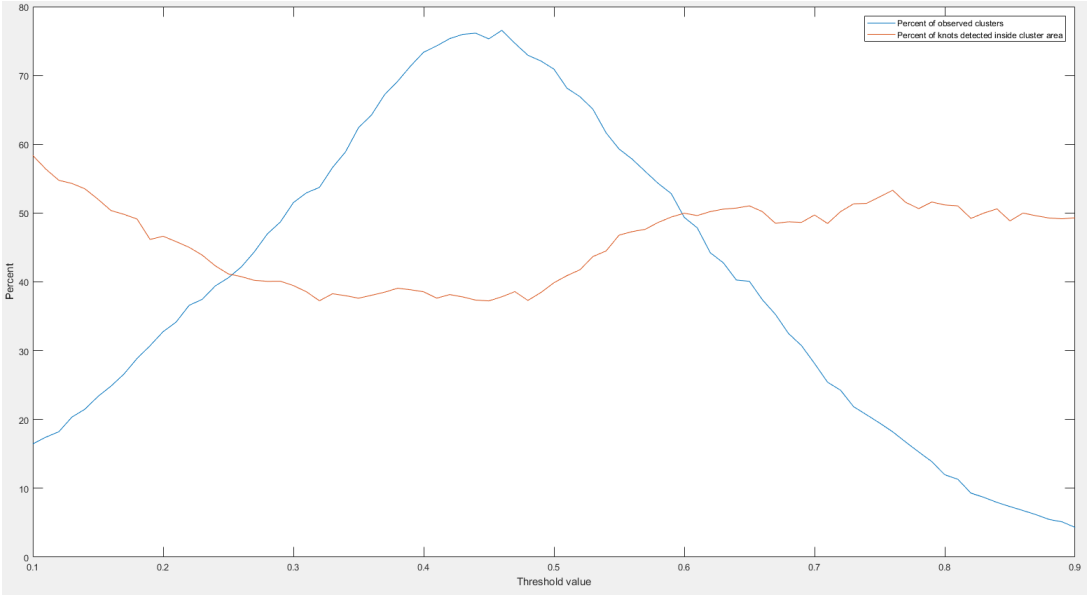

Figure 43. The dependence of knot detection parameters on the threshold value.

7 DISCUSSION

7.1 Current study

In this article, an application for detecting knots using the laser scanning data was described. The basic idea of the application was to transform point cloud model of a log into the 2-D log surface image. This image was used to highlight areas of protrusion from the log surface. Subsequently, among those areas, those with significant local surface rises were selected as probable knot positions.

The detected knot positions were verified using a data from X-ray scanning. The X-ray data describes positions of knot cluster areas on the log. Thus, two parameters were evaluated: the percentage of clusters in which the knots were found, and the percentage of knots found inside the cluster area. The average percentage of cluster areas with at least one bough is 71.1%, which indicates a good detection of knots confirmed by the X-ray scanning. The percentage of knots found inside the cluster area is 43.4%. This value indicates that more than half of the found knots are not a part of the knot clusters. This result is satisfactory, since it is not assumed that the log contains only knot clusters, without separately located knots. Also part of the surface rises, which were classified by the presented method as knots, may be caused by other log surface defects.

7.2 Future work

Since the topic of this paper is very extensive, there are several possibilities for its continuation. Two main following areas for further work were observed. First, it is possible to improve the described method by increasing the quality of the input data. For example, a point cloud can be made more accurately using a better laser scanner or implementing a special method of noise reduction. Also, information about the true structure, average width, and size of knots may increase the accuracy of knot detection. Also one of the possible improvements of the method is the expansion of the types of detected defects, for example wounds or holes.

Second direction of further work is the use of multimodal matching of wood data to track its state at different stages of production. The application of methods implies the multimodal matching of data of laser and X-ray scanning of logs with images of sawed boards. The basic matching element is the position of knots. The extract position of knot

inside log can be determined by the surface data from the laser scanning and the inner log data from the X-ray scanning. These knots can be compared with knots found on sawed boards. Thus, it may be possible to determine for each board its original log, evaluate the board quality by scanning the log and track the lifecycle of a raw material from the beginning to the end product.

The latest development of this project is a deepening in the study of the properties of the tree, with the aim of establishing the patterns of the appearance of knots on a log. An example of such projects is the study of the probability of finding a knot depending on its location on the tree trunk. So can be establish which part of the tree, the bottom or top, is the knotless. Or knots can be detected on the log surfaces of different species in order to determine what kind of wood is better suited for detecting knots on its surface, as well as what wood is less affected by knots.

8 CONCLUSION

In the thesis an application for knot detection by using 3-D laser scan data was described. The work contains the detailed formulation of the methods of tracking wood in the sawmilling enterprise. Various external defects of a debarked log were described, as well as methods for their detection by the laser scanning. In this study, the method of detecting knots using laser point cloud was developed. The method of obtaining the image of the log surface using the robust 2-D circle fitting to the log-data cross-sections was proposed. With the data from laser scanning only, the method confirmed the detection of over 71.1% of clusters of knots, the data on which were approximated by the X-ray scanning.

Also, the basic ideas of the multimodal matching were given in the thesis, which can be used in future works. This method allows to match data of the laser and X-ray scanning of log and images of the sawn boards. In the thesis were the ways of finding knots on logs and boards, as well as ways of matching them.

REFERENCES

[1] P. D. Dykstra, G. Kuru, R. Taylor, R. Nussbaum, B. W. Magrath, and J Story. *Technologies for Wood Tracking Verifying and Monitoring the Chain of Custody and Legal Compliance in the Timber Industry*. Discussion paper, Word Bank, Washington, DC, 2002.

[2] Digisaw research project. http://www2.it.lut.fi/project/digisaw/index.shtml, 2018. [Online; accessed May, 11, 2018].

[3] European Wood, China. http://www.europeanwood.org.cn/en/european-wood, 2018. [Online; accessed May, 11, 2018].

[4] Ring debarkers lift fiber recovery, profits. http://www.timberlinemag.com/articledatabase/view.a 2008. [Online; accessed May, 11, 2018].

[5] Timber automation. https://timberna.com/equipment/logpro-drum-debarker/, 2018. [Online; accessed May, 11, 2018].

[6] Oklahoma cooperative extension service. http://factsheets.okstate.edu/documents/fapc-148-basics-of-softwood-sawmilling/, 2018. [Online; accessed May, 11, 2018].

[7] Direct industry. http://www.directindustry.com/prod/segem/product-63783-853689.html, 2018. [Online; accessed May, 11, 2018].

[8] Peterson corp. http://www.petersoncorp.com/products/4810f-chain-flail-debarker/, 2018. [Online; accessed May, 11, 2018].

[9] N. K Huyler. Live-sawing: a way to increase lumber grade yield and mill profits. *U.S. Department of Agriculture Research Paper. Forest Service, Northeastern Forest Experiment Station*, 1974.

[10] H. Hallock, A.R. Stern, and D.W. Lewis. *Is there a best sawing method?* U.S. Department of Agriculture Research Paper. Forest Service, Forest Products Laboratory, 1987.

[11] SibirLes, Russia. http://www.sibirles.ru/catalog/radialnyj-raspil.html, 2018. [Online; accessed May, 11, 2018].

[12] S. Chiorescu and A Gronlund. The fingerprint approach:Using data generated by a 3D log scanner on debarked logs to accomplish traceability in the sawmill's log yard. *Forest Products Journal*, 54(12):269–276, 2004.

[13] S Chiorescu. *The Forestry - Wood Chain: Simulation Technique, Measurement Accuracy, Traceability Concept*. PhD thesis, Luleå University of Technology, 2004.

[14] R. Hietaniemi, S. Varjo, and J Hannuksela. A machine vision based lumber tracing system. In *The 8th International Conference on Computer Vision Theory and Applications (VISAPP 2013)*, pages 98–103, 2013.

[15] R. E Thomas. Modeling the relationships among internal defect features and external appalachian hardwood log defect indicators. *Silva Fennica*, 43(3):447–456, 2009.

[16] F. Longuetaud, F. Mothe, B. Kerautret, A. Krähenbühl, L. Hory, J. M. Leban, and I Debled-Rennesson. Automatic knot detection and measurements from x-ray ct images of wood: a review and validation of an improved algorithm on softwood samples. *Computers and Electronics in Agriculture*, 85:77–89, 2012.

[17] R. Norlander, J. Grahn, and A Maki. Wooden knot detection using convnet transfer learning. In *Scandinavian Conference on Image Analysis*, pages 263–274, 2015.

[18] C. Aguilera, M. Ramos, and A Sappa. Simulated annealing: A novel application of image processing in the wood area. In *Simulated Annealing - Advances, Applications and Hybridizations*, pages 91–104, 2012.

[19] F. Taylor, F. Wagner, C. McMillin, I. Morgan, and F Hopkins. Locating knots by industrial tomography. *Forest Product Journal*, 34:42–46, 1984.

[20] E. Johansson, T. Pahlberg, and O Hagman. Fast visual recognition of scots pine boards using template matching. *Computers and Electronics in Agriculture*, 118:85–91, 2015.

[21] Oliveira L. S. Koerich A. L. Cavalin, P. and A. S. Britto. Wood defect detection using grayscale images and an optimized feature set. In *32nd Annual Conference on IEEE Industrial Electronics (IECON)*, pages 3408–3412, 2006.

[22] Lijun S. Wenshu, L. and Jinzhuo W. Study on wood board defect detection based on artificial neural network. *The Open Automation and Control Systems Journal*, 7:290–295, 2015.

[23] H. Gu, I. Y.-H. Andersson and R Vicen. Wood defect classification based on image analysis and support vector machines. *Wood Science and Technology*, 44(4):693–704, 2010.

[24] L. Thomas, C. Shaffer, L. Mili, and E Thomas. Automated detection of severe surface defects on barked hardwood logs. *Forest Products Journal*, 57(4):50–56, 2007.

[25] L. Thomas and R.E Thomas. A graphical automated detection system to locate hardwood log surface defects using high-resolution three-dimensional laser scan data. In *17th Central Hardwood Forest Conference*, 2010.

[26] Schmoldt-D.L. Schad, K.C. and R.J. Ross. Nondestructive methods for detecting defects in softwood logs. *U.S. Department of Agriculture Research Paper. Forest Service, Forest Products Laboratory*, 1996.

[27] J. Skog. *TCharacterization of sawlogs using industrial X-ray and 3D scanning*. PhD thesis, Luleå University of Technology, 2016.

[28] Kerautret-B. Debled-Rennesson I. Longuetaud F. Krähenbühl, A. and F. Mothe. Knot detection in x-ray ct images of wood. In *8th International Symposium on Visual Computing*, pages 209–218, 2012.

[29] C. R. Lockard, J. A. Putnam, and R. D. Carpenter. *Log defects in southern hardwoods*. The United States Government Publishing Office, 1950.

[30] E. Thomas. Identifying external defects on logs. http://extension.umd.edu/sites/extension.umd.edu/files/_docs/programs/woodland-steward/IDing-External-Defects_Thomas.pdf, 2009. [Online; accessed May, 11, 2018].

[31] U Kretschmer, N. Kirchner, C. Morhart, and H. Spiecker. A new approach to assessing tree stem quality characteristics using terrestrial laser scans. *Silva Fennica*, 47(5):1–14, 2013.

[32] S.M. Stangle, F. Brüchert, U.H. Sauter, U. Kretschmer, and H. Spiecker. Clear wood content in standing trees predicted from branch scar measurements with terrestrial lidar and verified with x-ray computed tomography. *Canadian Journal of Forest Research*, 44(2):145–153, 2014.

[33] G. Hermosillo, C. Chefd'Hotel, and O Faugeras. Variational methods for multimodal image matching. *International Journal of Computer Vision*, 50(3):329–343, 2002.

[34] C. Zhao, H. Zhao, J. Lv, S. Sun, and B Li. Multimodal image matching based on multimodality robust line segment descriptor. *Neurocomputing*, 177:290–303, 2016.

[35] M Hutter. Distribution of mutual information. In *Advances in Neural Information Processing Systems 14*, pages 399–406, 2002.

[36] M. T. Heideman, D. H. Johnson, and C. S Burrus. Gauss and the history of the fast fourier transform. *IEEE Acoustics, Speech, and Signal Processing (ASSP) Magazine*, 1:14 – 21, 1984.

[37] C. Huang, H. Huang, H. Toyoda, T. Inoue, and H Liu. Correlation matching method for high-precision position detection of optical vortex using shack–hartmann wavefront sensor. *Optics Express*, 20:26099–26109, 2012.

[38] O. Zuniga and R.M Haralick. Corner detection using the facet model. In *International Conference on Pattern Recognition and Image Processing*, pages 30–37, 1983.

[39] W. Zhao, Zhao C., Y. Wen, and S Xiao. An adaptive corner extraction method of point cloud for machine vision measuring system. In *International Conference on Machine Vision and Human-machine Interface*, pages 80–83, 2010.

[40] Y. Wang, Ewert, D. D. Schilberg, and S Jeschke. Edge extraction by merging 3D point cloud and 2D image data. In *10th International Conference and Expo on Emerging Technologies for a Smarter World (CEWIT)*, page 1–6, 2013.

[41] J. Huang and S You. Point cloud matching based on 3D self-similarity. In *IEEE Computer Vision and Pattern Recognition (CVPR) Workshops*, pages 41–48, 2012.

[42] Z Zhang. Iterative point matching for registration of free-form curves and surfaces. *International Journal of Computer Vision*, 13(2):119 – 152, 1994.

[43] R.B. Rusu, N. Blodow, Z. Marton, M. Dolha, and M Beetz. Towards 3D Point cloud based object maps for household environments. *Robotics and Autonomous Systems*, 56(11):927–941, 2008.

[44] J. Woo, M. Stone, and J. L. Prince. Multimodal registration via mutual information incorporating geometric and spatial context. *IEEE Transactions on Image Processing*, 24(2):757–759, 2015.

[45] X. Yang, R. Kwitt, M. Styner, and M Niethammer. Fast predictive multimodal image registration. In *2017 IEEE 14th International Symposium on Biomedical Imaging (ISBI 2017)*, 2017.

[46] M. A. Fischler and R. C. Bolles. Random sample consensus: a paradigm for model fitting with applications to image analysis and automated cartography. *Communications of the ACM*, 24(6):381–395, 1981.

[47] W. Kaewapichai and P Kaewtrakulpong. Robust ellipse detection by fitting randomly selected edge patches. *World Academy of Science, Engineering and Technology International Journal of Computer and Information Engineering*, 2(12):4018–4021, 2008.

[48] B. A. Shenoi. *Introduction to digital signal processing and filter design*. John Wiley and Sons, 2006.

[49] G. Bianchi and G. Sorrentino. *Electronic filter simulation & design*. McGraw-Hill Professional, 2007.

[50] N. Otsu. A threshold selection method from gray-level histograms. *IEEE Transactions on Systems, Man and Cybernetics*, 9(1):62–66, 1979.

[51] S. P. Duraisamy and R. Kayalvizhi. A new multilevel thresholding method using swarm intelligence algorithm for image segmentation. *Intelligent Learning Systems & Applications*, 2:126–138, 2010.

[52] Chen-T.S. Liao, P.S. and P.C Chung. A fast algorithm for multilevel thresholding. *Journal of Information Science and Engineering*, 17:713–727, 2001.